Pathogenesis Induced by Tick-borne Encephalitis Virus in Epithelial Cells

DISSERTATION

zur Erlangung des akademischen Grades
doctor rerum naturalium
(Dr. rer. nat.)
im Fach Biologie
eingereicht an der
Lebenswissenschaftliche Fakultät
der Humboldt-Universität zu Berlin
von

M.Sc. Chao Yu

Präsident der Humboldt-Universität zu Berlin
Prof. Dr. Jan-Hendrik Olbertz

Dekan der Lebenswissenschaftliche Fakultät
Prof. Dr. Richard Lucius

Gutachter/innen:
1. Prof. Dr. Matthias Niedrig
2. Prof. Dr. Detlev H. Krüger
3. Prof. Dr. Friedemann Weber

Tag der mündlichen Prüfung: 01.10.2014

Der SINN erzeugt die Eins.

Die Eins erzeugt die Zwei.

Die Zwei erzeugt die Drei.

Die Drei erzeugt alle Dinge.

--------Tao Te King by Lao Tse

In memory of my father

In memory of my uncle

In memory of my grandfather

To my mother

To my wife

Selbstständigkeitserklärung

Ich erkläre hiermit, dass ich die vorliegende Arbeit selbstständig und nur unter Verwendung der angegebenen Hilfen und Hilfsmittel angefertigt habe. Alle Stellen, die wörtlich oder sinngemäß aus Quellen entnommen wurden, sind als solche gekennzeichnet. Abbildungen, die anderen Quellen unverändert entnommen oder diesen entlehnt wurden, sind mit der Quellenangabe versehen. Ich versichere, dass ich mich nicht anderweitig um einen Doktorgrad beworben habe oder einen entsprechenden Doktortitel besitze. Die Promotionsordnung der Lebenswissenschaftliche Fakultät der Humboldt-Universität zu Berlin habe ich gelesen und akzeptiert.

Berlin,

_____

Chao Yu

Declaration of Authorship

I certify that the work presented here is, to the best of my knowledge and belief, original and the result of my own investigations, except where acknowledged. The present work has not been submitted, either in part or whole, for a degree at this or any other University. Parts of this work have been or will be published under the following titles:

1. **Yu, C.**, K. Achazi, and M. Niedrig, *Tick-borne encephalitis virus triggers inositol-requiring enzyme 1 (IRE1) and transcription factor 6 (ATF6) pathways of unfolded protein response.* Virus Res, 2013. 178(2): p. 471-7.

2. **Yu, C.**, **K. Achazi**, M. Lars, JD. Schulzke, M. Niedrig, R. Bücker, *Tick-borne encephalitis virus replication, intracellular trafficking, and pathogenicity in human intestinal Caco-2 cell monolayers.* Plos ONE, accepted.

Berlin,

_____

Chao Yu

Abbreviations

µg	Microgram
µl	Microliter
µM	Micromolar
Abs	Antibodies
ATCC	American Type Culture Collection
BBB	Blood-brain barrier
bp(s)	Base pair(s)
BSA	Bovine serum albumin
CMC	Carboxy methyl cellulose
CPE	Cytopathic effects
Da	Dalton
DNA	Deoxyribonucleic acid
dNTP	Deoxyribonucleotide triphosphate
ds	double-stranded
E. coli	*Escherichia coli*
EEA1	Early endsome antigen-1
EDTA	Ethylenediaminetetraacetic acid
EIPA	5-(N-Ethyl-N-isopropyl)-amiloride
ER	Endoplasmic reticulum
EtBr	Ethidium bromide
FCS	Fetal calf serum
g	Earth’s gravitational acceleration
h	Hour(s)
HRP	Horse radish peroxidase

IFA	Immunofluorescence assay
IFNs	Type I interferons
IgG	Immunoglobulin G
kDa	Kilo Dalton
L	Liter
LB	Luria Bertani
M	Molar
mAb	Monoclonal antibody
min	Minute(s)
mL	Milliliter
mM	Millimolar
MOI	Multiplicity of infection
MTT	3-(4, 5-Dimethylthiazol-2-yl)-2, 5-diphenyl tetrazolium bromide
ng	Nanogram
nm	Nanometer
nt	Nucleotide(s)
pAb	Polyclonal antibody
PBS	Phosphate buffered saline
PBS-T	Phosphate buffered saline containing Tween 20
PCR	Polymerase chain reaction
pfu	Plaque forming units
pmol	Picomol
PRR	Pattern recognition receptor
RT- qPCR	Quantitative real-time PCR

RKI	Robert Koch Institute
RNA	Ribonucleic acid
rpm	Revolutions per minute
RT	Room temperature
ss	single-stranded
SNX	Sorting nexin-5
TER	Transepithelial electrical resistance
TLR3	Toll-like receptor 3
TUDCA	Tauroursodeoxycholic acid
U	Unit (of enzyme activity)
v/v	Volume per volume
w/v	Weight per volume

Abstract

Tick-borne encephalitis virus (TBEV) is one of the most important vector-borne viruses in Europe and Asia. The transmission mainly occurs by the bite of an infected tick. Consuming of rough milk products from infected livestock animals also occasionally cause TBE cases. The objective was to prove that TBEV is capable of infecting human intestinal epithelial cells via the alimentary route. Caco-2 cells were used to investigate the pathogenesis caused by TBEV. During TBEV infection Caco-2 monolayers showed morphological changes with significant vacuolization. Ultrastructural analysis revealed dilatation of the rough endoplasmic reticulum and further enlargement to TBEV containing caverns. Caco-2 monolayers showed an intact epithelial barrier with stable transepithelial electrical resistance (TER). Concomitantly, viruses were detected in the basolateral medium, taken up via a transcytosis pathway. TBEV cell entry was efficiently blocked with different inhibitors (EIPA, Cytochalasin D, Nocodazole, LY294002), suggesting that actin filaments and microtubules are important for PI3K-dependent endocytosis. Moreover, experimental fluid uptake assay showed increased intracellular accumulation of FITC-dextran containing vesicles and co-localization of TBEV with early endosome antigen-1 (EEA1) and with sorting nexin-5 (SNX5) could confirm macropinocytosis as trafficking mechanism. In the late phase of infection, further evidence was found for translocation of virus via the paracellular pathway. Thus, TBEV pathomechanisms in human intestinal epithelial cells and its transmission via the alimentary route were enlightened.

The endoplasmic reticulum (ER) stress response is an important conserved molecular signaling pathway. I investigated the effects of the two UPR signaling

pathways upon TBEV infection in Vero E6 cells. I showed that the amount of heat shock protein 72 increased in the course of TBEV infection. I then confirmed that TBEV infection activates the IRE1 pathway and ATF6 pathway. Finally, I examined whether inhibition of the IRE1 pathway has an effect on TBEV infection. These findings provide the first evidence that TBEV infection activates the two UPR signaling pathways. Moreover, inhibition of TBEV replication by UPR inhibitors may provide a novel therapeutic strategy against TBE.

Zusammenfassung

Das Frühsommer-Meningoezephalitis-Virus (FSMEV) ist eines der wichtigsten von Vektoren übertragenen Viren in Europa und Asien. Auch wenn die häufigste Übertragung durch den Stich einer infizierten Zecke erfolgt, kommt es immer wieder zu FSME Infektionen, die durch den Genuss von Rohmilchprodukten infizierter Tiere hervorgerufen werden. Das Ziel der Arbeit war nachzuweisen, dass das FSME-Virus in der Lage ist, menschliche intestinale Epithelzellen über die Nahrungsaufnahme zu infizieren. Es wurden Caco-2 Zellen verwendet um die Pathogenese des FSMEV zu untersuchen. Monolayer von Caco-2 Zellen zeigten nach Infektion mit FSMEV morphologische Veränderungen mit signifikanter Vakuolisierung. Ultrastrukturanalysen zeigten eine Ausdehnung des rauen endoplasmatischen Retikulums (ER) und zusätzlich Vergrößerungen/Ausweitungen zu FSME Virus haltigen Kavernen. Caco-2 Epithelzellenmonolayer zeigten eine intakte Barriere mit stabilem transepithelialem elektrischem Widerstand (TEER) auf. Daneben wurden Viren im basolateralem Medium entdeckt. Diese wurden über einen Tanscystose Pathway aufgenommen. Der Zelleintritt von FSMEV konnte durch verschiedene Inhibitoren wirksam blockiert werden (EIPA, Cytochalasin D, Nocodazole, LY294002), was darauf hinweist, dass Aktinfilamente und Mikrotubuli wichtig für die PI3K-abhängige Endozytose sind. Darüber hinaus zeigte die experimentelle Flüssigkeitsaufnahme erhöhte intrazelluläre Ansammlungen von FITC-Dextran haltigen Vesikeln und die Co-Lokalisation von FSME-Viren mit frühem Endosom Antigen-1 (EEA1) und mit sorting nexin-5 (SNX5). Dieses könnte die Makropinozytose als Transportmechanismus bestätigen. In der späten Phase der Infektion wurden weitere Hinweise für die

Translokation des Virus über den parazellulären Weg gefunden. Dadurch wurde Der FSMEV Pathomechanismus in menschlichen Intestinalepithelzellen und seine Übertragung über Nahrungsmittel näher aufgeklärt.

Die Stressantwort des endoplasmatischen Retikulums ist ein wichtiger konservierter „molecular signaling pathway“. Wir haben die Effekte der zwei UPR „signaling pathways“ während der FSMEV infektion in VeroE6 Zellen untersucht. Hierbei konnte gezeigt werden, dass die Menge von „heat shock protein“ 72 im Verlauf der FSMEV Infektion ansteigt. Damit wurde bestätigt, dass eine FSMEV Infektion den „IRE1 - und den ATF6 pathway“ aktiviert. Schlussendlich haben wir untersucht ob die Inhibition des „IRE1 pathway“ einen Effekt auf die FSMEV Infektion hat. Diese Ergebnisse liefern den ersten Hinweis darauf, dass eine FSMEV Infektion die beiden „UPR signaling pathways“ aktiviert. Daraus ergibt sich die Möglichkeit, dass die Inhibierung der FSMEV Replikation durch UPR Inhibitoren eine neuartige therapeutische Strategie gegen FSME sein könnte.

Contents

1. Introduction

1.1 Tick-borne encephalitis virus

Tick-borne encephalitis virus (TBEV) is an important arthropod virus, which belongs to the tick-borne encephalitis flavivirus group, genus *Flavivirus,* cause a series of human neural diseases (Lindquist & Vapalahti, 2008). The lipid-enveloped TBE virus particle has a spherical structure with a diameter approximately 50 nm (Mandl, 2005). The TBEV genome is an unsegmented, positive-sense RNA with about 11,000 nucleotide bases. It has only one ORF (open reading frame) which is used for synthesizing a polyprotein. This polyprotein contains several structural proteins (such as envelope glycoprotein E, capsid protein C) and several non-structural proteins (such as NS1, NS3, NS5) (Figure 1) (Mukhopadhyay, Kuhn, & Rossmann, 2005). The isolated TBE viral strains analyzed by phylogenetics can be further divided into three different subtypes: (i) the European TBEV subtype; (ii) the Siberian TBEV subtype; (iii) the Far Eastern TBEV subtype (Ecker, Allison, Meixner, & Heinz, 1999).

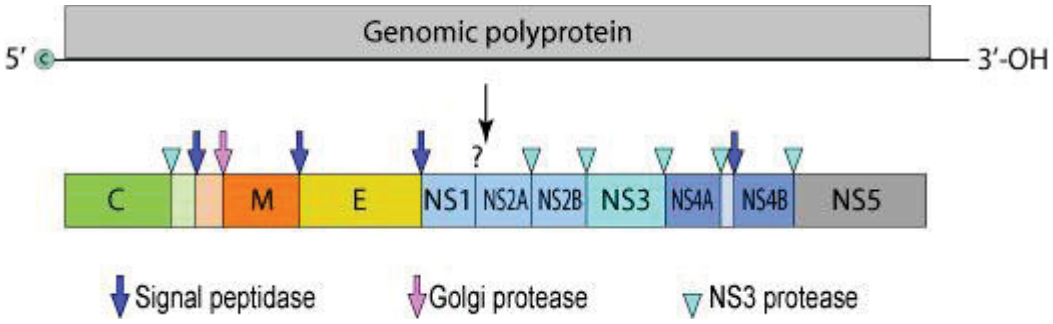

Figure 1. The representative structure of the TBEV genome and its polyprotein.
The whole TBEV genome which serves as messenger RNA is translated into several structural and non-structural proteins (adapted from ViralZone:www.expasy.org/viralzone, Swiss Institute of Bioinformatics).

1.2 TBEV replication and unfold protein response

1.2.1 TBEV replication

The diagram shows the typical TBEV life cycle and illustrates its individual replication steps (Figure 2). Initially, attaching to the molecules of the cell surface is pivotal for the virus entry into the host. During this course, it is mainly associated with the virus surface glycoprotein E containing the structure of ectodomain. The structure analyzed by the X ray crystallography showed that the architecture of ectodomain has the stem anchor dimers and facilitate to attach the cell membrane (Rey, Heinz, Mandl, Kunz, & Harrison, 1995).

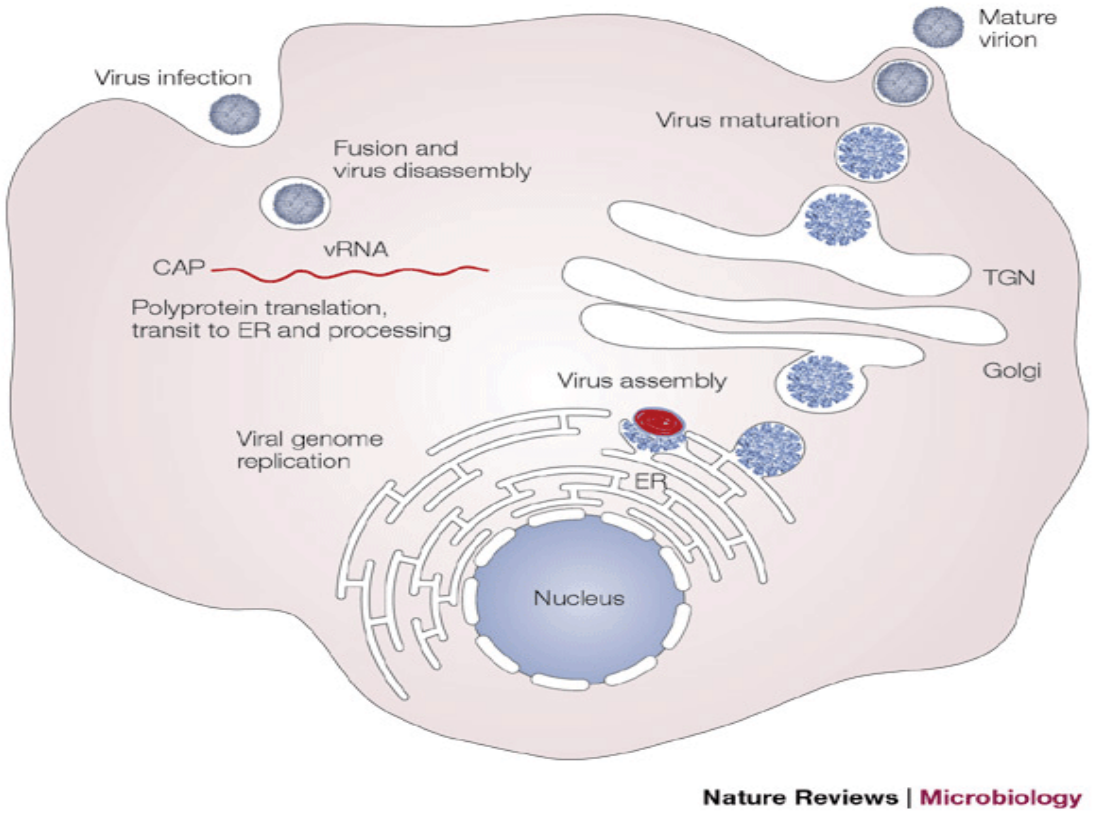

Figure 2. Schematic diagram of the TBE virus replication.
After attachment, the virions penetrate into the host by receptor-mediated endocytosis. Subsequently, the viral genome serves as the template for protein translation. After the assembly of the newly structural proteins and RNA on the membrane of ER, the immature virions are tranlocated through the TGN. Mature virions are finally released by the exocytic route. ER represents endoplasmic reticulum; TGN represents trans-Golgi network (adapted from (Mukhopadhyay et al., 2005)).

Although the exact cellular receptors for TBEV binding remain unclear, it is shown that glycosaminoglycan such as heparan sulphate, which is commonly expressed on various types of cells, assists virions via low-affinity on the cellular surface (Kozlovskaya et al., 2010; Mandl et al., 2001). Generally, many flaviviruses including dengue virus, West Nile virus diffuse the cells through receptor-mediated endocytosis by utilizing the pre-existing clathrin-coated pits. And then the virus was released into cytoplasm and transports into early endosome of the host cell (Kaufmann & Rossmann, 2011).

It is demonstrated that the microenvironment with low pH induces a rearrangement of the viral protein E structure to form homotrimer spikes which facilitate the fusion to the cellular membrane (Allison, Schalich, Stiasny, Mandl, & Heinz, 2001; Allison et al., 1995). Once the fusion develops, the released RNA genome in the cytoplasm serves as a template for protein translation. A polyprotein precursor is synthesized and then cleaved into a number of viral proteins by many proteases. The viral replication occurs on the reorganized membrane which provides a protection platform for yielding the newly positive-strand RNAs (Miorin et al., 2013). During virus assembly, immature particles are budded from the endoplasmic reticulum (ER) membrane and cleaved by protein prM (Elshuber, Allison, Heinz, & Mandl, 2003). And subsequently infectious virus are transported through the cellular exocytic pathway (Heinz et al., 1994).

1.2.2 Unfolded protein response

In every eukaryotic organism, the ER forms a membrane-enclosed network of tubules, vesicles, and cisternae, which provide many general functions such as synthesis and secretion of protein, production of lipid molecules and storage of chemical compounds (Lin, Walter, & Yen, 2008). However, the functions of ER are usually disrupted by mutated or unfolded protein during the process of many

viral infection diseases, which then cause ER stress (He, 2006). To oppose the ER stress, eukaryotic organisms employ several cellular counter-mechanisms. The unfolded protein response (UPR) is one of the most important signaling pathways which sense and regulate the ER stress. In the scenario of ER stress, the UPR signaling pathway is regulated by three major sensors which reside on the ER membrane. The three sensors are inositol-requiring enzyme 1 (IRE1), activating transcription factor 6 (ATF6), protein kinase RNA-like ER kinase (PERK) (Figure 3), respectively (Ron & Walter, 2007).

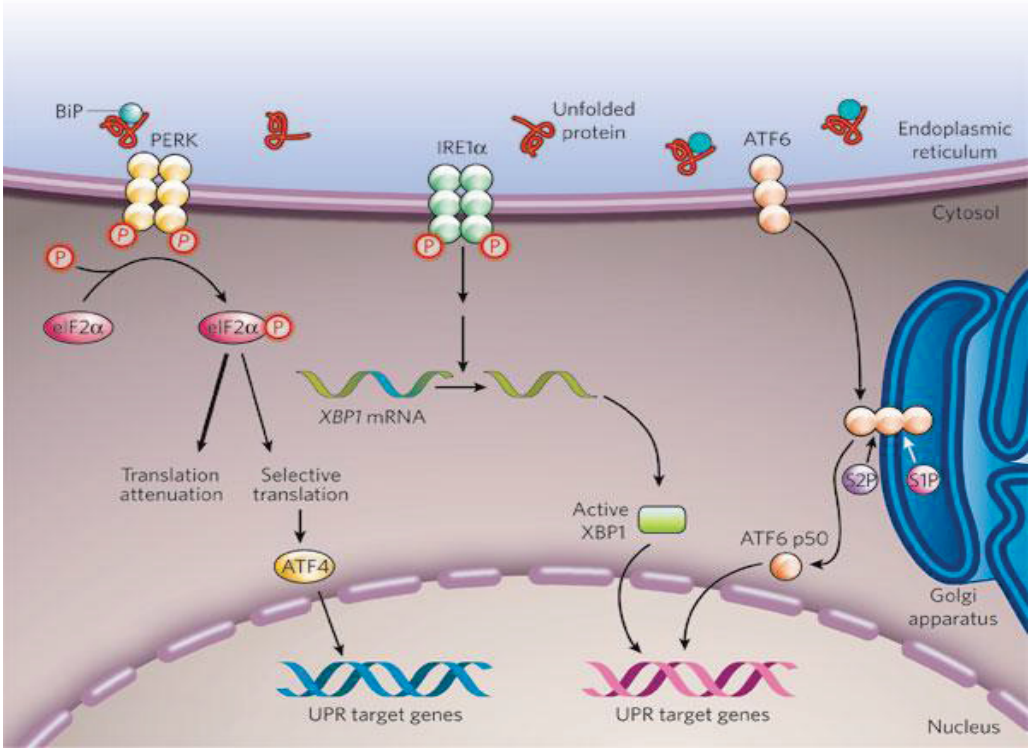

Figure 3. The three pathways of unfolded protein response.
Under ER stress, activation of UPR is governed by the initiators of IRE1α (inositol-requiring enzyme 1 alpha), PERK (protein kinase RNA-like ER) and ATF6 (activating transcription factor 6), respectively. Activation of PERK pathway, active PERK phosphorylates eIF2α (phosphorylates eukaryotic translation initiation factor 2α), reducing the overall protein synthesis. Activation of IRE1 pathway, a short intron belonged to the XBP1 (X-box-binding protein 1) mRNA is removed by IRE1α which yields active transcription factor spliced XBP1. Activation of ATF6 pathway, ATF6 moves to the Golgi body, which then split by the two proteases (S1P: site-1 protease, S2P: site-2 protease), producing the partial ATF6 (ATF6 p50). (adapted from (Zhang & Kaufman, 2008)).

In the course of PERK pathway, PERK phosphorylates eukaryotic translation initiation factor 2α (eIF2α) which then decrease the protein production (Harding, Zhang, & Ron, 1999). During activation of the ATF6 pathway, the active ATF6 moves to the Golgi apparatus which is processed by site-1 protease and site-2 protease. Then the fragment ATF6 is generated and migrates to the nucleus which modulate UPR genes (Ye et al., 2000). The IRE1 pathway is regulated by IRE1α and modulated by various regulators which named the UPRosome. The UPRosome contains a series of proteins, such as heat shock protein 72 (Hsp72), which locate at the ER membrane, (Hetz, 2012). Upon activation of the IRE1 pathway, the IRE1 cuts a 26bp nucleotides from the X box binding protein 1 (XBP1) mRNA which then produces the expression of the spliced transcription factor XBP1 (sXBP1). The sXBP1 then translocates to the nucleus and regulates the downstream activation (Yoshida, Matsui, Yamamoto, Okada, & Mori, 2001).

Until now, it has been demonstrated that many flaviviruses such as Japanese encephalitis virus (JEV), Dengue virus (DENV) facilitate their propagation in the host cells by triggering UPR pathways. During infection with JEV or DENV, the IRE1 pathway was preferentially activated and alleviated the cytotoxicity induced by virus (Umareddy et al., 2007; Yu, Hsu, Liao, & Lin, 2006). Whereas West Nile virus (WNV) manipulates IRE1 pathway, ATF6 pathway and PERK pathway which then increased the production of virus as well as inhibited the host antiviral capacity (Ambrose & Mackenzie, 2011). In addition, WNV or JEV infections induce cellular apoptotic response by increasing the expression of a transcription factor, CHOP protein (Medigeshi et al., 2007; Su, Liao, & Lin, 2002). The CHOP protein is a CCAAT/-enhancer-binding protein homologous which is involved in the cause of the UPR (Marciniak et al., 2004).

1.3 Vector and transmission of TBEV

At present, there have been nearly 900 tick species which documented and further divided into three groups. These groups are the Argasidae (soft ticks), the Ixodidae (hard ticks) and the Nuttalliellidae respectively (Pfaffle, Littwin, Muders, & Petney, 2013). Ticks act as the main vector which plays an important role in the TBEV transmission to the host. The European subtype virus is generally carried by the small hard tick *Ixodes ricinus*, which distributes across the many European countries (Medlock et al., 2013). The Far-eastern and the Siberian subtype virus are mainly transmitted by the *Ixodes persulcatus,* the taiga tick. This tick species is mainly distributed from Russian to Far-eastern Asia (Hayasaka et al., 2001). Consequently, the different subtypes of TBEV have been formed a long belt in the circulating areas (Figure 4).

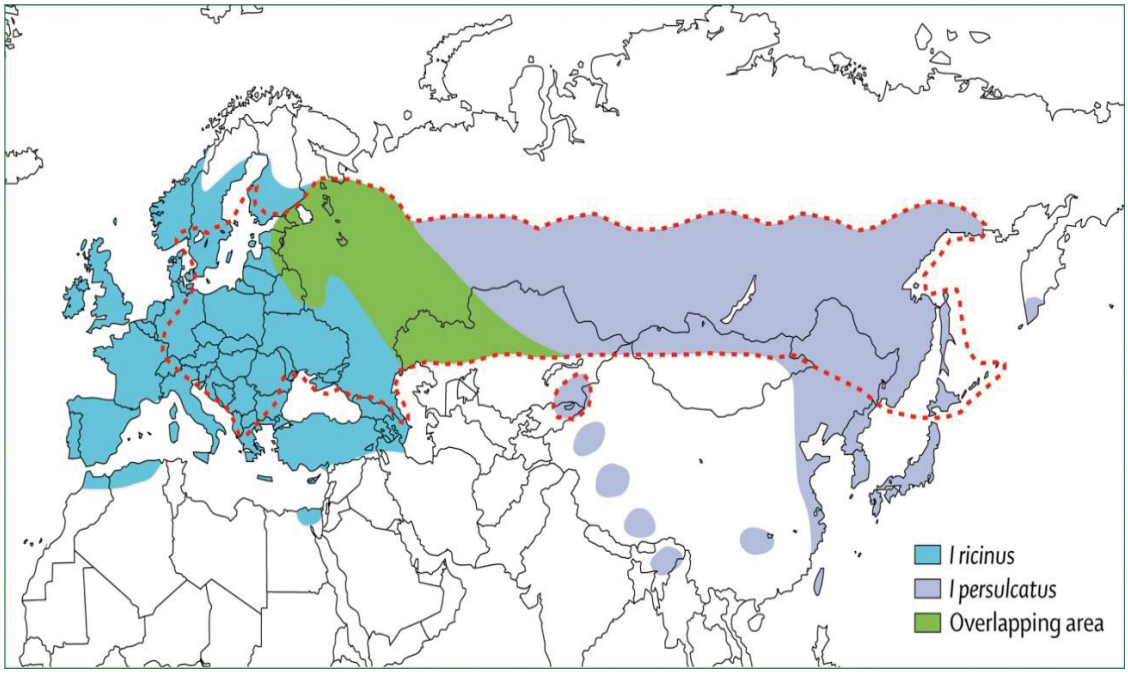

Figure 4. The distribution belt of TBE viruses in different species of ticks. The European subtype TBE virus is distributed in *Ixodes ricinus*, whereas the Far-eastern and the Siberian subtype TBE virus are carried by the *Ixodes persulcatus.* The green area indicates that the overlapped distribution of two vectors. The red dashed line shows the border of TBEV endemic region (adapted from (Lindquist & Vapalahti, 2008)).

Although a few present reports showed that the TBEV isolated from China (Si et al., 2011), Japan (Yoshii et al., 2011) and South Korea (Kim et al., 2009; Yun et al., 2011), the actual TBE infection distribution has to be investigated in the following days.

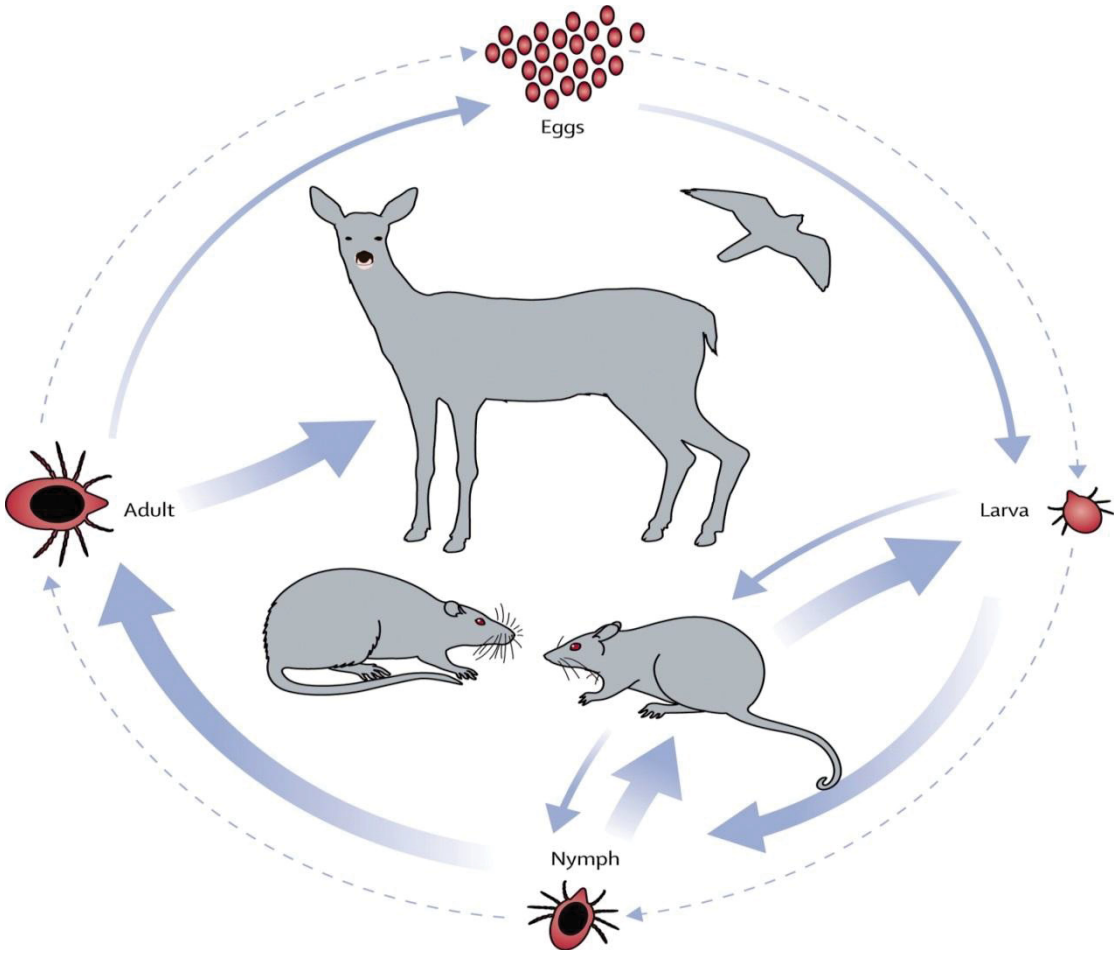

Figure 5. Transmission cycle of TBEV.
Clockwisely, the dotted arrows show that the whole lifespan of tick from eggs, larvae, nymph to adult. In the process of tick development, it requires blood meal provided by the host to develop into next stage. Moreover, adult females require blood meal to lay eggs. Solid arrows demonstrate that the TBE virus transmits to mammals by transstadially and transovarially (adapted from (Lindquist & Vapalahti, 2008)).

In general, tick life cycle has four stages which start from eggs, larvae, nymphs to adults (Figure 5). To employ the tick as a vector, TBE viruses have to adapt the life span of tick development. Therefore, TBE virus transmission occur

transstadially as well as transovarially. Moreover, each of individual stage can maintain for a long period of tick development until moving into the next stage under proper geographical environment, which facilitate to transmit the virus to a new host (Pfaffle et al., 2013). The small rodent is one of the most important mammal hosts and reservoirs for TBEV transmission (Bakhvalova, Potapova, Panov, & Morozova, 2009). These animals in the field are also used as sentinels for evaluating TBEV circulation in endemic areas (Achazi et al., 2011). Moreover, it is reported that in many investigations many wild animals (roe deer) and domestic animals (horses, dogs) also serve as hosts for virus transmission (Kiffner, Vor, Hagedorn, Niedrig, & Ruhe, 2012; Klaus, Horugel, Hoffmann, & Beer, 2013; Pfeffer & Dobler, 2011).

There are three routes which TBE virus transmission to humans (Figure 6). Under natural environment humans are usually infected with TBE virus via the bite of an infected tick when working at the vegetation or walking through the forest. The exhaled carbon dioxide or body heat from the mammal serves as stimuli for ticks questing (Gherman et al., 2012). The incidence of reported TBE cases increases in different countries and its spread to new regions are thought to depend on several possible reasons, such as socio-economic situation in various regions, modification of host expansion and habitat and geographic ranges at extremes of altitude and latitude (Medlock et al., 2013). The changes of climate are also associated with the abundance of ticks and virus transmission in endemic areas although it is difficult to predict the prevalence by climate model (Gray, Dautel, Estrada-Pena, Kahl, & Lindgren, 2009).

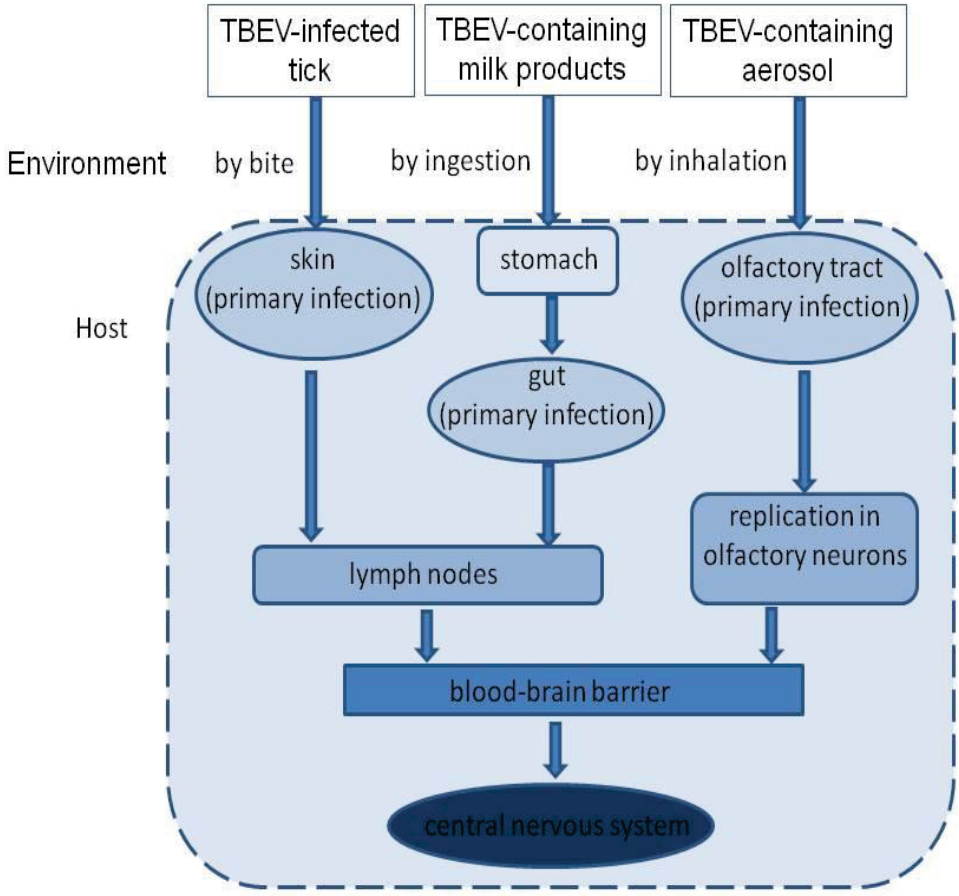

Figure 6. The overview of TBEV transmission to the human.
The TBEV transmission to human occurs by tick bite, ingestion of infectious milk products or inhalation of TBEV containing aerosol (modified from (Dorrbecker, Dobler, Spiegel, & Hufert, 2010)).

Another transmission of TBE virus results from the alimentary route by means of ingestion of raw milk or its related products. After drinking TBEV infected milk, it is rapidly emptied by the stomach and moved into the duodenum within few minutes while gastric acid is secreted in the stomach around 1h after consumption of the milk (Gritsun, Lashkevich, & Gould, 2003). Due to the TBE viruses maintain its infectivity for at least two hours in gastric acid, it is able to pass further the digestive tract without losing its infectivity (Pogodina, 1958). Moreover, the intestine consists of various cell types which could be effective

for supporting virus growth. Therefore, it was reasonable to assume that the human gastrointestinal tract is a beneficial environment for virus replication. This hypothesis was investigated in our experiments with human intestinal Caco-2 cells. Although the human TBE cases are caused by the infection of alimentary tract occasionally, recent publications have showed that more attention should be taken in many regions. In 2008 and 2012, several clinical TBE cases were reported due to eating goat cheese or drinking goat milk in western Austria and Slovenia (Holzmann et al., 2009; Hudopisk et al., 2013). In 2011, total 11 identified TBE cases in western Hungary were caused by consuming unpasteurised cow milk (Caini et al., 2012). Moreover, epidemiological investigation showed TBE virus was found by RT-PCR in milk samples from cows, goats and sheep, which indicated that consumption of raw milk have a high risk of infection in eastern Poland (Cisak et al., 2010). In addition, it has been experimentally proved that the infected goat yielded the TBE viruses in its milk with no clinical signs after 8 days post infection. Most importantly, the immunized goat did not produce TBE virus. This evidence could provide a potential way to avoid TBEV infection by consuming raw milk on the endemic regions (Balogh et al., 2012). Beside the conventional transmission by tick bite mentioned above, TBEV infections were accidentally occurred through needle-stick injuries when doing animal experiment with syringe. And transmission through inhaling infectious aerosol was also reported when culture flask with high amounts of virus were accidentally broken in the laboratory (Gritsun et al., 2003) .

1.4 Pathogenesis and Clinical manifestation of TBEV

After inoculation of TBE virus through an infected tick bite, many cell types like Langerhans cells and keratinocytes are initially infected and then activate the host innate immune responses (Labuda et al., 1996). In the course of this procedure, it is inevitable that host cellular receptors (pattern recognition receptors, PRRs) identify the specific molecular structures which are generally presented in most bacteria and viruses. The mainly types of PRRs include toll-like receptors, RIG-I-like receptors, etc. Among these PRRs, the family of TLRs contains the conserved pathogen binding domain and plays a critical response to the invading microorganisms (Janssens & Beyaert, 2003). A recent study has analyzed these mutations of TLR3 gene and OAS1 gene from the 128 patients with neural dysfunction caused by TBEV infection. The result indicates that the mutation of TLR3 gene is associated with TBEV infection, which might induce severe clinical manifestation (Kindberg et al., 2011). After ligand recognition by PRRs, the singling pathway of type I interferons (IFNs) is activated to mediate innate immune response. The induction of these cytokines provide the first line of host defense and facilitate to coordination and activation of other immune cells (Stetson & Medzhitov, 2006). Due to the potential antiviral effect of type I IFNs, Flaviviruses includes TBEV employ many strategies to counteract or decrease its production. In the case of Langat virus (a member of TBE complex virus) infection, expression of NS5 inhibited interferon-stimulated JAK-STAT signaling by blocking STAT1 phosphorylation (Best et al., 2005). Further study showed that NS5 protein interacts with the PDZ protein scribble (hScrib) which acted as antagonist for impairing interferon (IFN) response (Werme, Wigerius, & Johansson, 2008). Moreover, comparing different strains of TBEV infection to

induce IFNs, the expression of IFN transcripts mainly depended on the amounts of viral RNA (Overby, Popov, Niedrig, & Weber, 2010).

After the viruses get access to the nearby lymphatic nodules via lymphatic circulation, plasma viraemia is gradually developed by virus replication. During this phase, various organs (liver, spleen etc.) are infected and live viruses are produced which maintain viraemia for a few days (Haglund & Gunther, 2003) Finally, the viruses penetrate through the blood-brain barrier (BBB), then impair the neural tissues, which cause several clinical manifestations. The mouse model was used to investigate this neural pathogenesis of TBEV infection. After inoculation of TBEV in two mouse strains (BALB/c and C57Bl/6), the virus caused a substantial BBB disruption associated with the increased its permeability. At the later infection, the mice showed that the severe neurological signs with dramatic decrease in body weight and temperature. Meanwhile, the expression of proinflammatory cytokine/chemokine was upregulated in the brain, which may contribute the disease progression (Ruzek, Salat, Singh, & Kopecky, 2011). The data also indicated that the pathogenesis of TBEV infection in mice based on their genetic background. In another study, the identified mouse strains STS mice exhibited resistant to TBEV infection. Whereas the other two mouse strains (BALB/c and the CcS-11) displayed intermediate and high susceptible to TBEV infection, respectively. The result suggested that the genetic background has a great significance in the clinical TBE course (Palus et al., 2013). In addition, another investigation has demonstrated that the interaction between TBEV and neural cells. The cells including neuroblastoma, medulloblastoma etc. showed the susceptibility to TBEV infection, which then produced high amounts of virus titers. Most importantly, infected neural cells exhibited many morphological changes including apoptotic features (Ruzek et

al., 2009). Besides the mouse model, the goats were used and challenged with TBEV in the experiment. The study showed that no clinical symptoms were exhibited in the goats compared to the controls, although the TBE viruses were found in the milk from 8 to 19 days post infection (Balogh et al., 2012). Many studies on the pathogenesis of TBEV infection were performed, however, the detailed mechanism of TBEV caused neuroinvasiveness and neurovirulence in humans have to be further investigated in the future.

There is a variety of clinical outcomes that can be examined in the TBE patients. Most importantly, these clinical symptoms from mild to severe also depend on the different of TBEV subtype. In general, the Far Eastern subtype often destroys the neurologic tissue which causes meningoencephalitis or polyencephalitis. The percentage of fatality is around between 20% and 60%. The Siberian subtype causes chronic or progressive symptoms with a low ratio of fatality. And the European subtype produces milder disease which shows a biphasic course. After the tick bite, the average of the incubation period is regularly between 7 and 14 days. In the first phase, the typical symptoms are fever, headache, muscle aches, and fatigue etc. although nearly two thirds of infectious people are subclinical. In the second phase, the viruses invade the central nervous system which give rise to the several neurological diseases including aseptic meningitis, encephalitis, or myelitis (Haglund & Gunther, 2003). Compared with different symptoms presented in humans, other hosts including horse, dog, goat etc. normally did not show any manifestations even with high seroprevalence in the population (Klaus et al., 2012; Roelandt et al., 2011; Rushton et al., 2013).

1.5 Vaccination and prevention

Due to no particular antiviral treatment for TBE, inoculation of human TBE vaccine provides the most efficient protection against virus infection. At present, several certified TBE vaccines are used by a large number of people and marketed in the different countries. Two vaccines come from Russia, which are TBE-Moscow (produced by Chumakov Institute) as well as EnceVir (produced by Microgen) (Leonova & Pavlenko, 2009), two others are licensed in Europe which are FMSE-Immune (Baxter, Austria) and Encepur (Novartis, Germany) (Heinz, Holzmann, Essl, & Kundi, 2007). And one vaccine is produced by Changchun Institute of Biological Products, China (Lu, Broker, & Liang, 2008). These vaccines are manufactured by different isolated strains including the far-eastern strains Sofjin and strain 205 (Heinz et al., 2007), the European subtype strains Neudorfl (Austria) and strain K23 (Germany) (Charrel et al., 2004), and the Chinese SengZhang strains (Lu et al., 2008). Similarly, all TBE vaccines are developed from the purified virus with formaldehyde inactivation and ultracentrifugation. Generally, the immunisation schedule contains injection of 3 vaccine doses. The second vaccine is administered between 1 to 3 months after the first. The last vaccine is administered between 9 to12 months.

Previous investigation in Austria demonstrated that TBE vaccination offers a high field effectiveness of protection (approximate 99%) among regularly vaccinated people at difference age of groups (Heinz et al., 2007). Another protective effect was evaluated the antibodies from 290 persons who were immunized with different TBE vaccines. According to the neutralization test, the results showed that all four vaccines provide a high and durable level of seroconversion, especially the Encepur vaccine (100%). More importantly,

different types of vaccine were administered to the same person also offered a high and sustainable protection. (Leonova & Pavlenko, 2009). In addition, the neutralizing antibody induced by vaccination with FMSE-Immune provides a potent cross-protection against the three subtypes of TBE viruses: European, Far Eastern, and Siberian (Orlinger et al., 2011). This phenomenon provides more convenient choice when conducting vaccination in different endemic areas or against unknown subtype of TBE virus.

Recently many reports showed several milk-borne TBE cases in the patient infected by oral route due to consuming unpasteurized cow or goats' milk (Caini et al., 2012; Holzmann et al., 2009; Hudopisk et al., 2013). This kind of infection could be efficient avoided by the pasteurization of infected milk or its products (Balogh et al., 2012). However, many persons preferred to consume unpasteurized milk influenced by the healthy and natural lifestyle. And also some people insistently believe that drinking raw milk is beneficial for curing many human diseases. Therefore, immunization of animals in the TBEV endemic regions and educational efforts of advising people to consume pasteurized milk would avoid the risk of infection.

In addition, with the large amount of people to do outdoor activities in the countryside and travellers to walk through the rural forests, careful examination together with proper clothing (for example, long sleeved shirt and long trousers) could be utilized in order to avoid the tick bite. Meanwhile, tick repellent could be sprayed on the exposed skin for personal protective measures although the effectiveness is time limited and its application still needs further investigation in the future (Vazquez et al., 2008). If a tick is examined to be bite to the skin, fine-tipped tweezers should be used to grasp the tick and removed it immediately to avoid jnfection by tick transmitted diseases.

1.6 Aims of study

While the infection route via tick bite has been elucidated in great detail, little is known about the alimentary route of infection in the molecular level. To achieve this purpose, the first main objectives of study thus were:

I. To investigate the TBEV pathogenesis in human intestinal Caco-2 cells

II. To analyze the cellular uptake mechanism during TBEV infection in Caco-2 cells

Additionally, although the effect of many flaviviruses on different UPR pathways has been investigated, the role of TBEV infection in cellular UPR is still unknown. The second main goal of our study was to analyze the role of the UPR, in particular regarding the IRE1 pathway and ATF6 pathway in the course of TBEV infection.

2. Materials and methods

2.1 Materials

Table 1. Chemicals and reagents

Product	Manufacturer
4',6-Diamidino-2-phenylindol (DAPI)	Invitrogen, Darmstadt, Germany
3,5-Dibromosalicylaldehyde	Sigma-Aldrich, Deisenhofen, German
5-(N-Ethyl-N-isopropyl)-amiloride	Sigma-Aldrich, Deisenhofen, German
Acti-stain™ 488 phalloidin	Cytoskeleton, inc. Denver, USA
Bovine serum albumin (BSA)	Carl Roth, Karlsruhe, Germany
Carboxymethylcellulose (CMC)	Carl Roth, Karlsruhe, Germany
Cytochalasin D	Sigma-Aldrich, Deisenhofen, German
Dimethylsulfoxide (DMSO)	Serva, Heidelberg, Germany
Ethanol	Carl Roth, Karlsruhe, Germany
Formaldehyde (37 %)	Carl Roth, Karlsruhe, Germany
2-Mercaptoethanol	Sigma, St. Louis, USA
Triton X-100	Sigma, St. Louis, USA
FITC-dextran (Molecular Weight 70 000 Da)	Sigma-Aldrich, Deisenhofen, German
HEPES	Carl Roth, Karlsruhe, Germany
LY294002	Sigma-Aldrich, Deisenhofen, German
Nocodazole	Sigma-Aldrich, Deisenhofen, German
Sodium chloride (NaCl)	Merck, Darmstadt, Germany
Sodium hydroxide (NaOH)	Carl Roth, Karlsruhe, Germany
Sucrose	Merck, Darmstadt, Germany
Tetracycline hydrochloride	Sigma, St. Louis, USA
Triton X-100	Sigma, St. Louis, USA

Trizma® hydrochloride (Tris-HCl)	Sigma, St. Louis, USA
Trizma®Base (Tris-Base)	Sigma. St. Louis, USA
TUDCA	Calbiochem, Darmstadt, Germany
Tween 20	Sigma-Aldrich, Deisenhofen, German
UltraPure™ Agarose	Invitrogen, Darmstadt, Germany

Table 2. Buffers and solutions

Buffer/ Solution	**Ingredients**
Phosphate buffered saline (PBS)	8.0 g NaCl, 0.2 g KCl, 1.44g Na2HPO4, add 1 L ddH2O
CMC overlay medium	1 g naphthol blue black, 13.6 g sodium acetate, 60 mL glacial acetic acid, add 1 L ddH2O 1.6 g carboxymethylcellulose in D-MEM with 1 % L-glutamine, 1% P/S and 10 % FCS
fixation buffer (plaque assay)	100 mL 37 % formaldehyde in 900 mL PBS
Naphthalene Black (Staining solution)	1 g of naphthol blue black, 13.6 g of sodium acetate, 60 mL of glacial acetic acid and up to 1 L of ddH_2O
Luria-Bertani medium (LB)	10 g Bacto-tryptone, 5 g Bacto-Yeast extract 5 g NaCl, adjust pH to 7.5 with NaOH, autoclave, cool to 55°C and add antibiotics suitable for the expression plasmid
Triton buffer	0.1% Triton-X100 in PBS
Blocking buffer I	PBS, 5 % (w/v) BSA
Blocking buffer II	5% non-fat milk in PBS solution with the

	Tween 20
Washing buffer	PBS, 0.5 % (v/v) Tween 20

Table 3. Cell lines

Cells	Description	Source
A549 cells	Human alveolar basal epithelial cells	ATTC: CCL-185
Caco-2 cells	Human intestinal epithelial cells	ATCC: HTB-37
VeroE6 cells	African green monkey kidney cells	ATCC: CRL-1586
PS cells	Pig, kidney cells	RKI

ATCC: *American Type Culture Collection*

Table 4. Cell culture

Product	Manufacturer
Cell culture flasks Nunclon™Δ Surface (25-175 cm^2)	Nunc™, Wiesbaden, Germany
CryoTubes™ (1 mL and 1.8 mL)	Nunc™, Wiesbaden, Germany
Nunc Multidishes Nunclon™ Δ (24 and 96 wells)	Nunc™, Wiesbaden, Germany
Falcon tubes (15 mL and 50 mL)	TPP,Trasadingen, Switzerland
D-MEM culture medium	Gibco BRL®, Eggenstein, Germany
E-MEM culture medium	Gibco BRL®, Eggenstein, Germany
Fetal calf serum (FCS)	PAA, Pasching, Germany
L-glutamine	PAA, Pasching, Germany
1:2 mixture of Trypsin / EDTA	PAA, Pasching, Germany
Penicillin and streptomycin solution	PAA, Pasching, Germany

Table 5. TBE virus strains

Virus strain	Source
K23	RKI
Sofjin	RKI
Aina	RKI

Table 6. Kits

Product	Manufacturer
BCA protein assay kit	Pierce, Rockford, USA
NE-PER nuclear extraction kit	Pierce, Rockford, USA
RNeasy total RNA isolation kit	Qiagen, Hilden, Germany
RNeasy Mini Kit	Qiagen, Hilden, Germany
Thermoscript First-Strand Synthesis System	Invitrogen, Darmstadt, Germany
Supersignal West Femto Maximun Sensitivity Substrate	Pierce, Rockford, USA
RNA viral kit	Qiagen, Hilden, Germany
Plasmid kit	Qiagen, Hilden, Germany

Table 7. Agarose gel electrophoresis

Product	Manufacturer
6x Loading Dye	Fermentas, St. Leon-Rot, Germany
GeneRuler™ 100bp DNA-Ladder	Fermentas, St. Leon-Rot, Germany
EtBr	Carl Roth, Karlsruhe, Germany
Agarose (NuSieve®3:1)	Biozym, Oldendorf , Germany

Table 8. PCR

Product	Manufacturer
Platinum® *Taq* DNA- Polymerase	Invitrogen™, Karlsruhe, Germany
10x PCR buffer	Invitrogen™, Karlsruhe, Germany
MgCl2	Invitrogen™, Karlsruhe, Germany
dNTP (Deoxyribonucleotide trlukaell)	Amersham, Freiburg, Germany
PCR water (DNase-free, Fluka)	Sigma-Aldrich, Deisenhofen, Germany

Table 9. Software

Product	Manufacturer
ABI 7500 Sequence Detection Software V2.0.6	Applied Bioscience, Foster City, USA
Adobe Photoshop CS6	Adobe Systems Incorporated, San Jose, USA
EndNote X7	Thomson Reuters, New York, USA
GraphPad Prism 5.0	GraphPad Software, San Diego, USA
Image J V1.42d	Wayne Rasband, NIH ,USA
ZEN 2009	Carl Zeiss GmbH, Germany

Table 10. Instruments

Product	Manufacturer
NanoDrop™ ND-1000 Spectrophotometer	PeQ Lab, Erlangen, Germany
Infinite® 200 PRO microplate reader	Tecan Group Ltd., Männedorf, Switzerland
Electronic Chop stick	(EVOM, World Precision Instruments, FL, USA)
BioPhotometer	Eppendorf, Hamburg, Germany
Thermomixer comfort	Eppendorf, Hamburg, Germany
Fast Semi-Dry Blotter	Pierce, Rockford, USA
Light microscope	Keyence Corp, Japan
Confocal laser-scanning microscope	Zeiss LSM510, Jena, Germany

Table 11. Primary antibody

Product	Manufacturer
ATF6	Abcam, Cambridge,UK
EEA1	BD Bioscience, CA, USA
TBEV E protein	RKI
XBP1	Santa Cruz Biotechnology, CA, USA
β-actin	Cell Signaling Technology, Frankfurt am Main, Germany

Table 12. Secondary antibody

Product	Manufacturer
Alexa 594-labeled anti-mouse IgG antibody	Invitrogen, Darmstadt, Germany
FITC-labeled anti-mouse antibody	Caltag Laboratories, Hamburg, Germany
FITC-labeled anti-rabbit antibody	Caltag Laboratories, Hamburg, Germany
IgG mouse HRP conjugated	Cell Signaling Technology, Frankfurt am Main, Germany
IgG Rabbit HRP conjugated	Cell Signaling Technology, Frankfurt am Main, Germany

2.1.1 Cell subculture

2.1.1.1 Maintenance and subculture routine

Both Vero E6 cells and A549 cells were seeded in Dulbecco's modified Eagle's medium (DMEM) with fetal bovine serum (10%), L-glutamine (1%) and mixture of penicillin (1%) and streptomycin (1%). Two kinds of cells were maintained in the incubator (37°C, 5% CO_2). Caco-2 cells were maintained at 37°C and 5%

CO_2 and grown in minimal essential medium (MEM) with fetal bovine serum (10%), L-glutamine (1%) and mixture of penicillin (1%) and streptomycin (1%).

2.1.1.2 Polarized Caco-2 cells culture

For polarized Caco-2 cells culture, Caco-2 cells were cultured in the cell culture filters with a growth surface of 0.33 cm^2 and with 0.4 μm pore size. Media was replaced every 2 days. Experiments were performed with cells showing a transepithelial electrical resistance (TER) above 300 $\Omega \cdot cm^2$.

2.1.1.3 Cell preservation and recovery

Cells were trypsinated and harvested from sub-confluent cell monolayer (80%-90% confluence). The cell concentration was calculated by a hemacytometer under light microscope. Next, the cell suspension was manipulated by centrifugation at 310×g for 10 min. After discard the supernatant, the resuspension of cell pellet was performed in the cold freeze medium. The final concentration was $2\text{-}4\times10^6$ cells/ml. Then the cells were transfered into special tube as 1 mL per tube. Finally, the tubes were moved into the freezer (-20°C) for approximate 30min and then placed to a -80°C refrigerator for a long storage.

2.1.1.4 Cell number calculation

The number of cells in the suspension was counted under light microscope with a haemocytometer. Briefly, pipette approximately 10μl cell suspension at the edge of the cover-slip and allow to flow under the cover slip. And then cells in four large squares were calculated. The number of cells counted was multiplied by proportion of ¼ x volume of dilution x 10^4 to calculate the original cell concentration (cell number per milliliter).

2.2.2 Virological methods

2.2.2.1 Virus propagation

Vero E6 cells were used for cultivating three different strains of TBE viruses K23, Aina and Sofjin as shown in the prior publication (Achazi et al., 2012). Briefly, viruses were inoculated at a MOI of 1 onto Vero E6 monolayer, which cultured in DMEM added with fetal calf serum (10%), L-glutamine (1%) and mixture of penicillin (1%) and streptomycin (1%). The supernatants were collected after 3 to 5 days. The TBE virus titer was calculated by the method of plaque assay as described below. All TBE viruses were used as a MOI of 1 for infection experiments unless otherwise indicated. K23 virus was selected as a prototype for three TBEV strains.

2.2.2.2 Plaque assay

To determine the viral titers in a given virus suspension, the plaque assay was used. A549 cells were seeded in the 24 well cell culture plate and were maintained in the incubator (37°C, 5% CO_2) overnight. Three viral suspensions were serially diluted and plused to each well. After 1 h incubation each well was filled with 500 µl carboxymethylcellulose (CMC) overlay medium and then the plates were put back and continually kept in the CO_2 incubator at 37°C. After 4 days, all wells were fixed with formaldehyde. After 1h each well was covered with the solution of Naphthalene Black. Plaques were counted and the viral titers were calculated and expressed as plaque-forming units/ml (pfu/ml). The calculation method is as below: pfu/ml was calculated by the plaque number multiplied by reciprocal of dilution factor and reciprocal of volume in mL

2.2.3 Viral infection and inhibitor assays

For infection studies, Caco-2 cells were cultured in the 24 well cell culture plate and inoculated with one of the three TBEV strains (MOI of 0.1). Then the plate was incubated for 1h at 37°C. Unbound virus was removed off by PBS and the plate was returned to the incubator at 37°C. Cellular viral RNA was collected and viral titers in the supernatants were determined at different time points by means of real-time quantitative RT-PCR and plaque assay.

For viral inhibition assays, the pharmacological inhibitors cytochalasin D (Cyt D), nocodazole (Noc) and LY294002 (LY) were diluted in DMSO and working concentrations were as follows: Cyt D at 2µM, Noc at 10µg/ml and LY at 10µM. DMSO treatment (0.1% DMSO in medium) without any inhibitor was used as control. Moreover, 5-(N-Ethyl-N-isopropyl)-amiloride (EIPA) was diluted with DMSO and concentrations used for the experiments were 0µM, 25µM and 50µM, respectively. To analyze the effects of the inhibitors on TBEV entry, Caco-2 cells were pre-treated with the different inhibitors for 30 min. Then the cells were infected with TBEV strain K23 either with or without the appropriate inhibitor in the incubator. After incubation for 1h, the cells were washed with PBS to remove unbound viruses. The cells were then harvested for extracting total RNA followed by translation into cDNA. Thus, viral RNA was detected by RT-qPCR.

For ER stress inhibition assays, the UPR inhibitors IRE1 and TUDCA were used. The IRE1 inhibitor has the salicylaldehyde form of the salicylaldimine and inhibits the IRE1 endoribonuclease activity specifically (Volkmann et al., 2011). TUDCA is a derivative of an endogenous bile acid that alleviates ER stress (Berger & Haller, 2011). Vero E6 cells were pre-treated for 1h with 60µM IRE1

inhibitor or 500µg/ml TUDCA. Vero E6 cells pre-treated with culture medium were used as control. Then all samples were inoculated with TBEV for another hour. Subsequently, cells were washed with PBS to remove the unbound virus particles and were further incubated in the presence of the inhibitors. After 24h and 48h post infection, virus-containing cell culture supernatant was analyzed by plaque assay and viral protein from lysed cells was detected by western blotting, respectively.

2.2.4 PCR

2.2.4.1 RNA extraction

For total RNA extraction, Qiashredder/Rneasy columns were used to purify the cellular RNA. All steps were performed followed the manufacturer's guideline.

2.2.4.2 Determination of RNA concentration

The NanoDrop™ ND-1000 Spectrophotometer was used to calculate the nucleic acid concentration. A ratio of A260/A280 from 1.8 to 2.0 showed a good quality of the nucleic acids.

2.2.4.3 cDNA synthesis

Using the Superscript II kit, cDNA was synthesied from cellular RNA and followed the below conditions.

Table 13. PCR reaction mixture and thermal conditions

20µl reaction mixture		Thermal condition	
PCR water	8µl	Temperature	Duration
5xRT buffer	4µl	65°C	10min
dNTPs (25 mM)	1,6µl	On ice	5min
Random primer(100ng/µl)	0,4µl	37°C	60min
DTT (0,1M)	0,5µl	93°C	5min

Superscipt II	0,5µl	4°C	Stop
Sample volume	1 µl		

2.2.4.4 Conventional PCR

PCR mixture was prepared with the XBP1 primer pairs below (Samali, Fitzgerald, Deegan, & Gupta, 2010), GAPDH was selected as a reference control (Kurisaki et al., 2003) (Table 14). For positive control, cells were treated with 1µg/ml Tunicamycin (TM) for 12h. TM is used for inhibiting the N-linked protein glycosylation under ER stress. The cycling was performed on the PCR instrument followed by these conditions: 5min at 95°C; 35 cycles of 30s at 95°C, 30s at 58°C and 30s at 72°C; 7 min at 72°C (Table 15).

Table 14. List of oligonucleotides used for PCR

Name	Sequence
XBP1 forward primer	TTACGAGAGAAAACTCATGGCC
XBP1 reverse primer	GGGTCCAAGTTGTCCAGAATGC
GAPDH forward primer	CCCATGTTCGTCATGGGTGT
GAPDH reverse primer	TGGTCATGAGTCCTTCCACGATA

Table 15. PCR reaction mixture and cycler conditions

25µl reaction mixture		Cycling condition		
PCR water	17,95µl	Temperature	Duration	Cycle number
10 × PCR buffer	2,5µl	95°C	5min	1X
$MgCl_2$ (50 mM)	0,75µl	95°C	30s	35X
dNTPs (25 mM)	2µl	58°C	30s	
Forward primer	0,5µl	72°C	30s	
Reverse primer	0,5µl	72°C	7min	1X
Taq polymerase	0,2µl	4°C	Stop	
Sample volume	1 µl			

The products of amplification were separated by electrophoresis on a 3% agarose gel and visualized by ethidium bromide staining. Images were photographed by Chemidoc system (Bio-Rad) and analysed by ImageJ software.

2.2.4.5 RT-qPCR

RT-qPCR amplification was fulfilled with the following primers (Table 16). The final reaction volume was 25µl with different amounts of component. The cycling condition was 95 °C for 5min, then 45 cycles for 15s at 95°C and 30s at 60°C (Table 17). GAPDH (Applied Bioscience) was used as a reference. Data analysis was used by comparative C_T method.

Table 16. List of oligonucleotides used for RT-qPCR

Name	Sequence
TBEV forward primer	TggAYTTYAgACAggAAYCAACACA
TBEV reverse primer	TCCAgAgACTYTgRTCDgTgTggA
probe	FAM-CCCATCACTCCWgTgTCAC-MGB-BBQ

Table 17. RT-qPCR reaction mixture and cycler conditions

25µl reaction mixture		Cycling condition		
PCR water	12,05µl	Temperature	Duration	Cycle number
10 × PCR buffer	2,5µl	95°C	5min	1X
$MgCl_2$ (50 mM)	2,5µl	95°C	15s	45X
dNTPs (25 mM)	2µl	60°C	30s	
Primer F	1,5µl			
Primer R	1,5µl			
Probe	0,5µl			
10× Rox	0,25µl			

Taq polymerase	0,2µl	
Sample volume	2µl	

2.2.5 Western blotting

2.2.5.1 Sample preparation

After washing with ice-cold PBS, the cells were lysed on ice with RIPA buffer (50mM Tris-HCl, pH 8.0, 0.1% SDS, 1% NP40, 150mM NaCl, 20% glycerol, 2mM dithothreitol with 0.5% deoxycholate acid). To harvest, the NE-PER nuclear protein extraction kit was used for harvesting nuclear proteins, followed the manufacturer's recommendations.

2.2.5.2 Determination of protein concentration

The Pierce™ BCA protein assay kit was used to determine the protein concentration. After measurement, all samples were stocked at -80°C until used.

2.2.5.3 SDS page and western blotting

The same amounts of cellular lysates or nuclear proteins were loaded on the 4% to 20% Tris-HEPES gels and run for electrophoretic separation. After electrophoresis, the gels were washed with pure water on the shaker for 15min. Then a semi-dry blotter was used for transferring the proteins onto the PVDF membranes. Subsequently, the membranes were washed with the blocking buffer II for 1h and labelled with primary antibodies (diluted from 1:500 to1:1000) at overnight in a cooling room (4°C). Anti-TBEV E protein antibody was utilized for examining the TBE virus (Niedrig et al., 1994). Anti-actin was applied for detecting the ß actin. Anti-PCNA (Proliferating cell nuclear antigen) antibody was used for examining and PCNA. Anti-XBP1 was used for detecting the XBP1 protein. Anti-ATF6 was used for detecting the partial ATF6. After

incubation, the membranes were washed with PBS solution (0.5% Tween 20) and labelled with the proper enzyme conjugated secondary antibody in the blocking buffer for 1h. Protein of interest was examined by applying the SuperSignal West Dura Extended Duration reagent and imaged under the Chemidoc system.

2.2.6 Microscopy

2.2.6.1 Light microscopy

Caco-2 cells were grown on the glass coverslips. Then the cells were infected with K23 virus and fixed with 3.7% formaldehyde at 24h, 48h or 72h post infection. All samples were photographed under the light microscope.

2.2.6.2 Indirect immunofluorescence microscopy

Caco-2 cells or Vero E6 cells were seeded on the glass coverslips. The cells were then infected with TBE viruses. At different time post infection, samples were briefly washed with PBS and fixed in formaldehyde. After 1h, all samples were permeabilized with 0.1% Triton X-100 and then incubated with blocking buffer. For detecting the envelope protein of the TBEV (E protein), the coverslips were treated with mouse monoclonal anti-TBEV E antibody (1:1,000) (Niedrig et al., 1994). And then the Alexa 594-labeled (1:200) or FITC-labeled (1:500) anti-mouse antibody was used for staining as the secondary antibody. For detecting the Hsp72 protein, samples were incubated with anti-Hsp72 (1:200). After 1h incubation, all of the coverslips were washed with PBS and then stained with TRITC labelled anti mouse antibody (1:200) as the secondary antibody. Cell nuclei were labelled by the 4’,6-diamidino-2-phenylindole (DAPI). All preparations were observed under the fluorescence microscope. The captured pictures were analysed using ImageJ software.

2.2.6.3 Confocal immunofluorescence microscopy

For analyzing the actin filament re-arrangement induced by TBEV infection, Caco-2 cells were stained with Acti-stain™ 488 phalloidin at 24h post infection. For detecting co-localization of TBEV E protein with the endosomal marker proteins EEA1 or SNX5 in infected cells, Caco-2 cells were stained with the mouse monoclonal anti-TBEV E protein antibody. Then the samples were stained with Alexa 594-labeled anti-mouse antibody (1:200) for 1h. EEA1 or SNX5 was stained with anti EEA1 or SNX5 antibody and FITC-labeled anti-rabbit antibody was used as the secondary antibody.

For monitor of ATF6 translocation, Vero E6 cells were infected with K23 virus for 24h after plasmid transfection. For the positive controls, the cells were incubated with TM (1 µg/ml) for 8h. All samples were then put in formaldehyde for fixation. After 1h, samples were incubated with 0.1% Triton X-100 buffer for permeabilization. Finally, all samples were treated with mouse monoclonal anti-TBEV E protein antibody (1:500) and then stained with an Alexa 594-labeled anti-mouse antibody (1:200). The Nuclei was stained by DAPI and samples were visualized by confocal laser-scanning microscope.

2.2.6.4 Ultrathin section transmission electron microscopy

Caco-2 cells infected with TBEV- were processed according to previously description and detected under ultrathin section transmission electron microscope (Laue, 2010). Sections of epon-embedded samples were post-stained with uranyl acetate and lead citrate. Samples were observed using the Jeol transmission electron microscope (JEM-2100) operated at 200 kV. Photographs were taken with a CCD camera at a resolution of 2k x 2k pixel.

2.2.7 Other methods

2.2.7.1 MTT assay for cell viability

Vero E6 cells or Caco-2 were cultured in the 96-well plate overnight and then the culture medium was removed. Vero E6 cells were treated with a series of concentrations two different inhibitors (TUDCA and IRE1 inhibitor) for 24h and 48h. The 20μl solution of 3-(4, 5-Dimethylthiazol-2-yl)-2, 5-diphenyl tetrazolium bromide (MTT) was added to each well. Then the cells were continually kept for 4h at 37°C. Finally, the medium was discarded and 200μl DMSO was added with gently shake for dissolving the formazan crystals. The absorbance was determined at 570nm by the spectrophotometer.

2.2.7.2 Apoptosis detection assay

To analysis the apoptosis, coverslips were taken at different time point post infection and fixed with formaldehyde. After PBS washing, the samples were permeabilized in the 0.1% Triton X-100 buffer (10min). After briefly washing with PBS, The apoptotic cells were examined by TUNEL assay following the manufacturer's recommendations. Nuclei were counterstained with DAPI. As positive control, samples were incubated with DNase I (3000U/ml diluted in 50mM Tris-HCl, pH 7.5, 1mg/ml BSA) (10min) under room temperature. All samples were examined under fluorescence microscope.

2.2.7.3 FITC-Dextran fluid uptake assay in Caco-2 cells

The cells were plated on the glass coverslips until getting confluent. After 4h TBEV infection, the cells were treated with FITC-dextran (Fdx) (Molecular Weight 70 000Da, Sigma-Aldrich) (final concentration, 0.5mg/ml) in the absence or presence of TBEV. After 30min the coverslips were washed with PBS and subsequently fixed. Simultaneous acquisition of FITC fluorescence emission

and transmitted light from all samples was done by confocal laser-scanning microscopy. Vesicle count was done by ImageJ particle analysis tool with fluorescence intensity threshold of Caco-2 monolayers where no Fdx was added.

2.2.7.4 TER measurement of TBEV in Caco-2 monolayers

Caco-2 cells were seeded on the insert with the 0.33cm^2 area and the 0.4μm pore size. After treatment of Caco-2 monolayers with the TBEV (MOI of 1) for 1h, fresh culture medium was replaced and TER of each transwell was determined every 24h using an epithelial volt ohmmeter with a pair of chopstick electrodes (Figure 7). Untreated monolayers were used as negative controls. In the course of virus infection, the same aliquots of medium were collected from the lower chambers at different time points as indicated. In addition, TBEV in the medium were detected using the RT-qPCR method as described above.

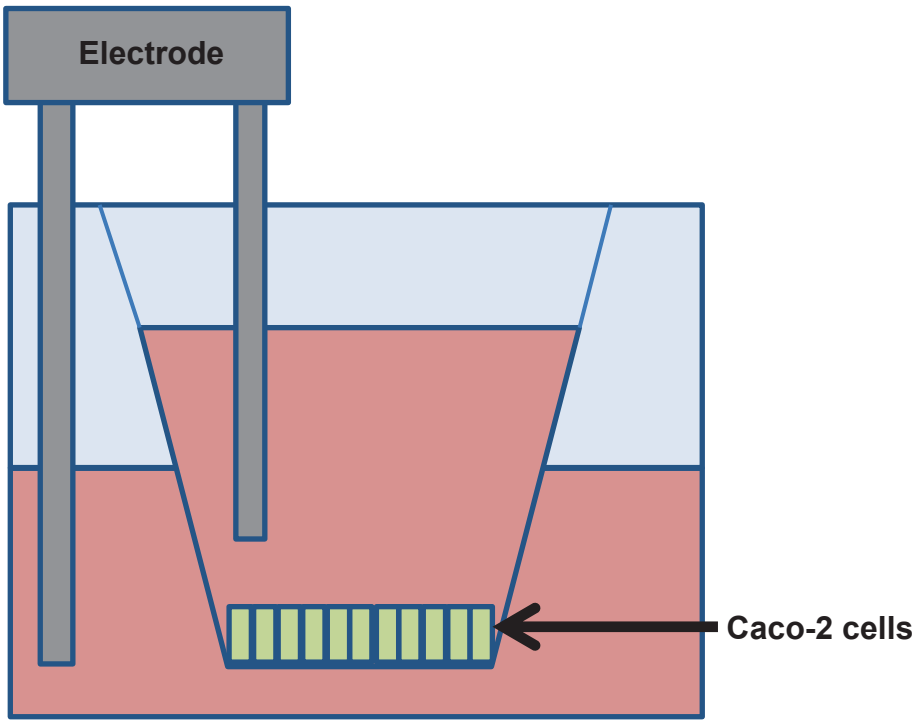

Figure 7. Animation of TER measurement.

Monolayers permeability was monitored by measuring the transepithelial electrical resistance (TER).

2.2.8 Statistical analysis

Statistical tests were carried out using Prism5 software (GraphPad, San Diego, Canada). Differences between treatment and control groups were compared using the Student's t-test. With a *P*-value of <0.05, the results were considered statistically significant.

3. Results

3.1Tick-borne encephalitis virus replication, intracellular trafficking, and pathogenicity in human intestinal Caco-2 cell monolayers

3.1.1 TBEV replication in human intestinal Caco-2 cells

Caco-2 cells were challenged with TBEV strain K23, Sojin, or Aina at a MOI of 0.1. Intracellular viral RNA was analyzed by RT-qPCR. Viral copy numbers of the three strains increased at the first day of infection, peaked at day 2 post infection (p.i.) and persisted in high amounts in the cells up to day 5p.i. (Figure 8A).

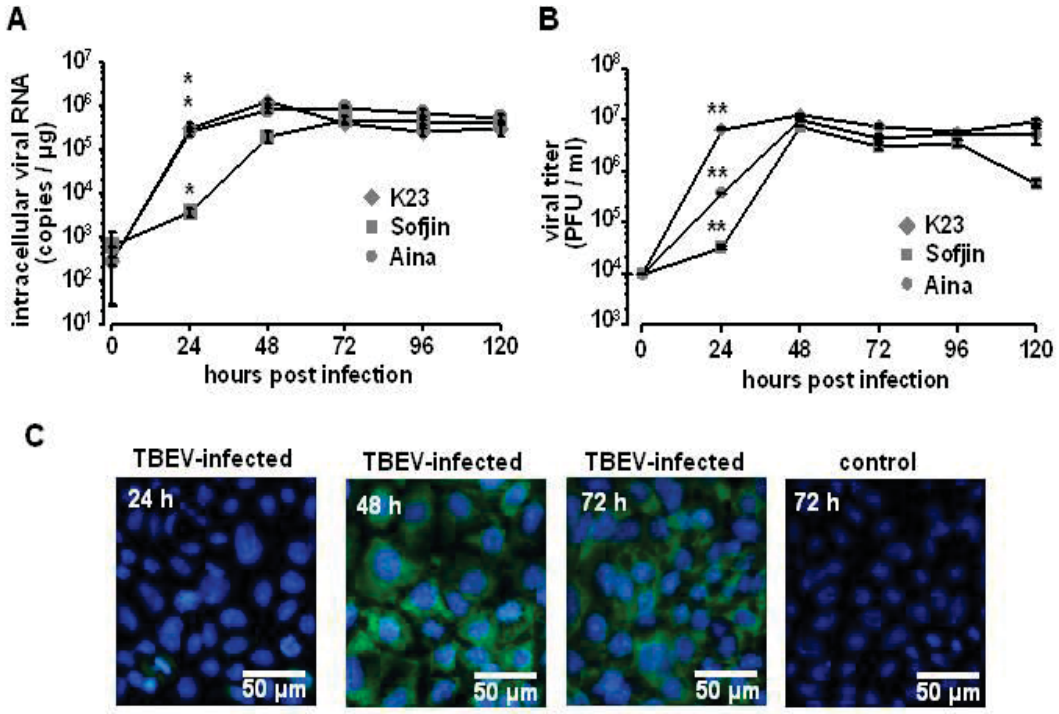

Figure 8. TBEV replication in Caco-2 cells.
Human cells infected with TBEV strains K23, Sofjin, and Ania at a MOI of 0.1. Viral supernatant and intracellular viral RNA were harvested at 24h, 48h, 72h, 96h and 120h p.i. **(A)** Intracellular TBEV RNA copy numbers, measured by RT-qPCR. **(B)** Viral titers in the supernatant determined by plaque assay, n=3; **P* < 0.05, ***P* < 0.01 to initial virus titer in Student's *t* test. **(C)** Immunofluorescence assay of TBEV-infected Caco-2 cell monolayers. Caco-2 cells infected with TBEV K23 strain were fixed at different time points and subjected to immunofluorescence assay. TBEV E (green), nuclei (blue, DAPI = 4'-6-diamidino-2-phenylindole dihydrochloride). One representative image of a triplicate is shown. Bar = 50 µm.

The amount of released TBEV particles in cell culture supernatant was highest on day 2p.i. for all 3 TBEV strains (Figure 8B). The virus titer in the apical cell supernatant increased by 3 log numbers between day 1 and 2.

We further monitored TBEV infection in Caco-2 cells with TBEV strain K23 by immunofluorescence microscopy. As shown in Figure 7C nearly 100% of the cells were found TBEV-positive at 48h p.i., while only few cells were positive at 24h p.i. This rapid virus spread between cells confirmed that TBEV replication is efficient in human intestinal Caco-2 monolayers and that the cells in general are susceptible to TBEV infection.

3.1.2 Cytological changes induced by TBEV infection in Caco-2 cells

In the course of TBEV infection in Caco-2 cells, a typical cytological changes accompanied by vacuolization was found, whereas morphological changes such as aggregation and shrinkage of cells or detachment of the monolayer were not observed at 48h p.i. (Figure 9). TBEV-induced vacuolization in infected Caco-2 cells was detected by immunofluorescence microscopy using anti-TBEV E monoclonal antibody at 24h, 48h, and 72h p.i. (Figure 9).

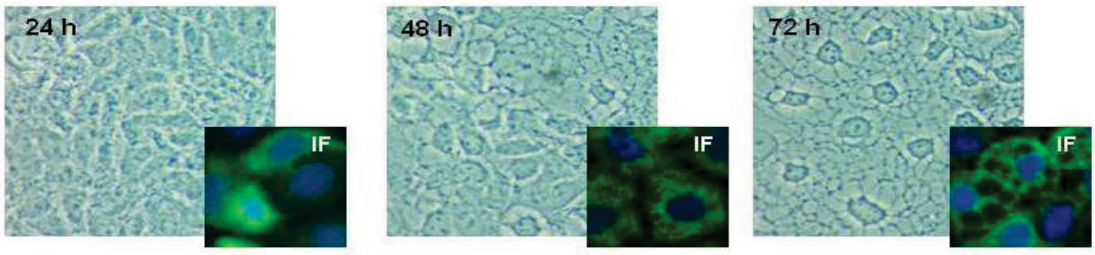

Figure 9. Cytological changes induced by TBEV infection.
Caco-2 cells were infected with TBEV K23 virus. Cellular morphological changes and vacuolization were monitored by light microscopy. Caco-2 cells were infected with TBEV strain K23 and fixed at 24h, 48h and 72h. Cells were observed with the 40x objective (400x total magnification). Details of cytoplasmic vacuolization are visualized by immunofluorescence (IF) microscopy. Samples were incubated with anti-TBEV E antibody and then stained with secondary anti-mouse antibody conjugated with FITC (green). The cell nuclei were stained with DAPI (blue).

3.1.3 Ultrastructural analysis of TBEV-infected Caco-2 cells

We analyzed the ultrastructural changes induced by TBEV infection in Caco-2 cells using ultrathin section transmission electron microscopy. A dilatation of the rough endoplasmic reticulum (rER) and presence of virus particles in rER cisternae were the first ultrastructural signatures of virus replication. At later stages large membrane-bound caverns in the cytoplasm contain most of the observed virions. The cavern membrane was coated with ribosomes indicating that it derived from the rER (Figure 10).

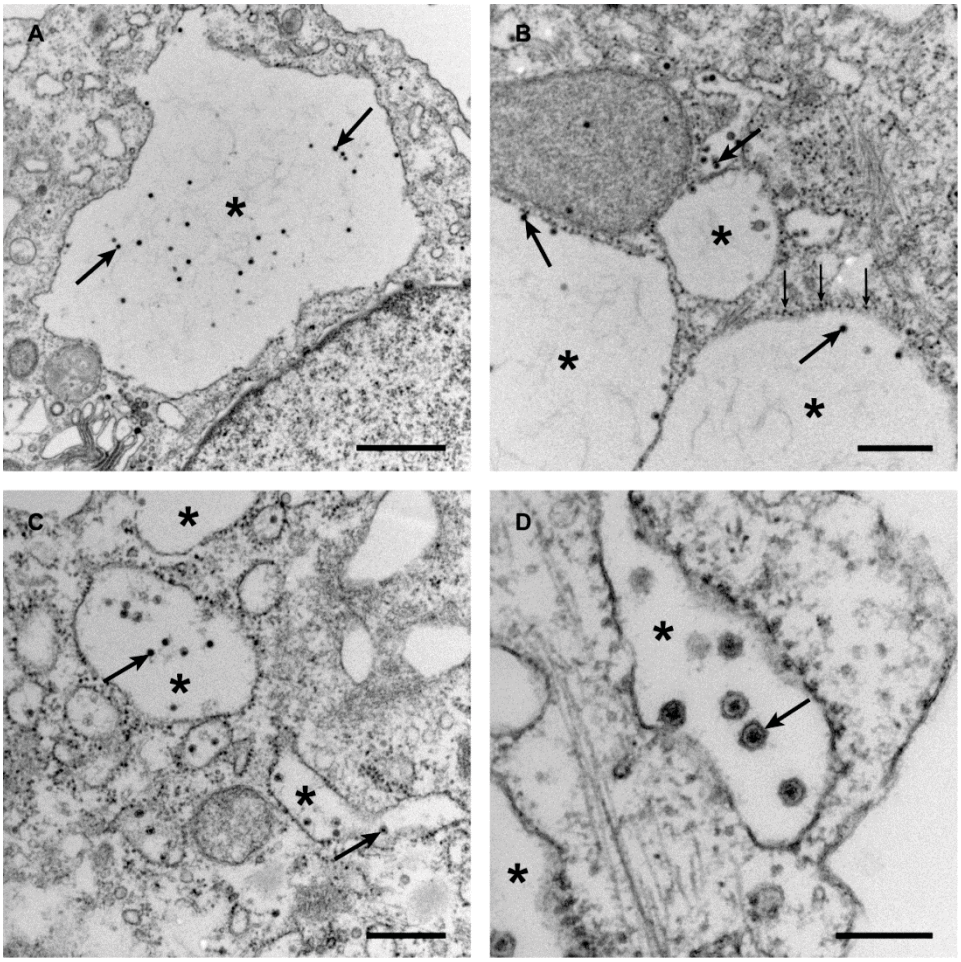

Figure 10. Ultrastructural analysis of TBEV-infected Caco-2 cells by ultrathin section transmission electron microscopy.
All photographs were taken at 12h p.i. where most of the virions could be observed. Representative virus particles are indicated by diagonal arrows. Caverns of the dilated rough endoplasmic reticulum (rER) containing TBEV are indicated by asterisks and ribosomes of the rER are indicated by small vertical arrows. (A) bar = 1µm, (B) bar = 500 nm, (C) bar = 500 nm, (D) bar = 200 nm.

3.1.4 Cytoskeletal changes and inhibition of virus entry

Initial cytoskeletal changes were observed 24h p.i. The actin cytoskeleton showed a general re-arrangement and more condensed microfilaments were observed than non-infected controls (Figure 11A). To test the response of the cytoskeleton to virus entry, we conducted inhibition experiments with inhibitors of cytoskeletal actin (cytochalasin D), microtubules (nocodazole) or autophagy/endocytosis via PI3-Kinase (LY294002).

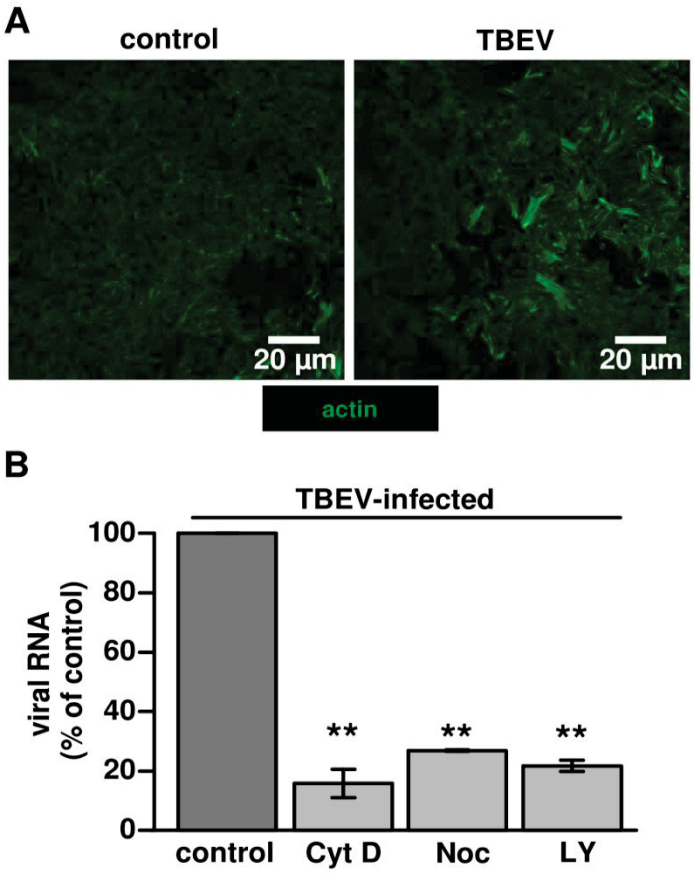

Figure 11. Cytoskeletal integrity is important for TBEV infection in Caco-2 cells.
(A) Actin re-arrangements following TBEV infection. Cells infected with TBEV strain K23 were fixed at 24h. Samples were stained for actin microfilament and the apical cell–domain (perijunctional cytoskeleton) was visualized by fluorescence microscopy with Acti-stain™ 488 phalloidin. Non-infected cells were used as controls. Bar = 20µm. **(B)** Microfilament blocking experiments on TBEV cell entry. Caco-2 cells were treated with cytochalasin D (Cyt D), nocodazole (Noc) or LY294002 (LY) for 30 min. DMSO treated Caco-2 cells were used as control. All samples were then infected with TBEV strain K23 for 1 h. Virus entry was monitored by RT-qPCR, n=3; $^{**}P < 0.01$.

All inhibitors induced a reduction in intracellular virus entry (Figure 11B). Since actin is required for the formation of plasma membrane ruffles in macropinosome formation as well as for trafficking of macropinosomes into the cell (Mercer & Helenius, 2009), we hypothesized that TBEV entry is mediated by a macropinocytosis-like mechanism.

3.1.5 TBEV entry into Caco-2 cells shows characteristics of macropinocytosis

The use of amiloride and its more potent derivative EIPA (5-(N-Ethyl-N-isopropyl)-amiloride) block the epithelial sodium channel (ENaC) as well as dose-dependently several other Na^+/H^+ antiporters. EIPA has often been used as a hallmark inhibitor that specifically inhibits endocytosis via the macropinocytic pathway (Koivusalo et al., 2010). As shown in Figure 12A, TBEV entry into Caco-2 cells is inhibited by EIPA treatment in a dose-dependent manner. One characteristic of macropinocytosis is the nonselective uptake of large amounts of extracellular solutes (Mercer & Helenius, 2009). To further investigate the involvement of macropinocytosis in TBEV entry, the uptake of soluble FITC-labeled dextran (Fdx) into Caco-2 cells was monitored. Fdx has often been applied as a morphological marker for macropinosomes and is used in fluid uptake assays (Figure 12B). We found that TBEV infection slightly increased the uptake of Fdx into Caco-2 cells from 166±79 vesicles and a total particle area of 5±2μm^2 in mock control versus 1138±101 vesicles with a total particle area of 60±4μm^2 ($p<0.01$ and $P<0.001$ respectively; n=3) in a high-power field of 135μm^2 in TBEV infected cells (Figure 12C).

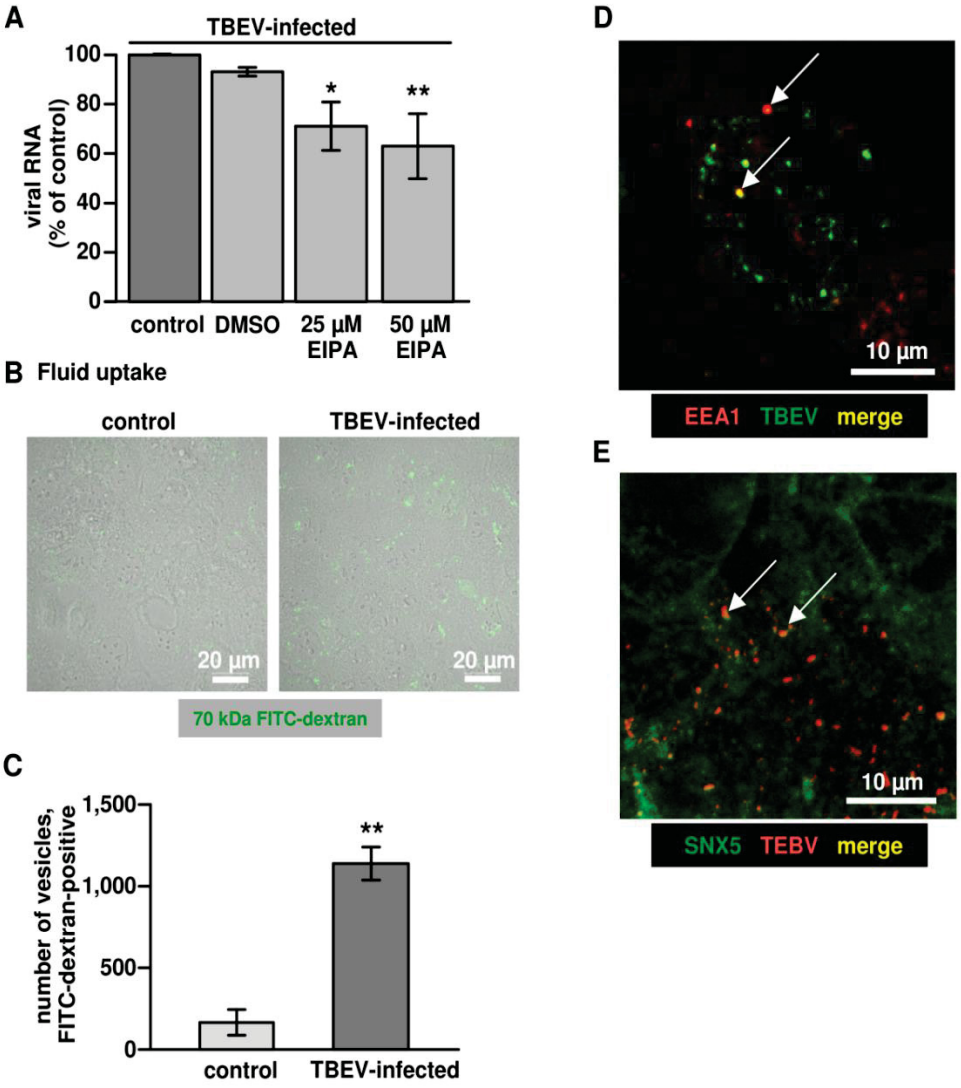

Figure 12. TBEV infected Caco-2 cells display characteristics of macropinocytosis.
(A) EIPA treatment impairs TBEV entry. Dose-dependence of EIPA-induced inhibition of TBEV entry. Caco-2 cells were pre-treated with EIPA for 30min, followed by incubation with TBEV in the presence of the inhibitor. After 1h, virus entry was monitored by RT-qPCR. n=3; **P* < 0.05, ***P* < 0.01. **(B)** Fluid uptake. Accumulation of intracellular FITC-dextran (green) induced by TBEV infection. Caco-2 cells were infected with TBEV strain K23 1h and then washed with PBS. Subsequently, cells were incubated with FITC-labeled dextran (1mg/ml). After 4h, cells were washed, fixed and observed by confocal microscopy. Bar = 20µm. **(C)** Accumulation of dextran in cells was analyzed by counting the total number of macropinocytic vesicles relative to the area occupied by the cell. ***P* < 0.01. **(D)** Immunofluorescence microscopy. TBEV co-localization (as merge in yellow, indicated by arrows) with early endosomal antigen-1 (EEA1) or **(E)** Sorting nexin-5 (SNX5) after virus entry. Cells were fixed and stained for TBEV anti-E protein and EEA1 or SNX5 with primary antibodies, followed by secondary antibodies as indicatedin the image. A representative image with a 63x objective is shown. Yellow dots as merge indicated representative examples of TBEV particles in co-localization with EEA1 or SNX5.

The average particle size of 0.04±0.01µm^2 in control was not different from Fdx vesicles in TBEV-infected Caco-2 monolayers with 0.06±0.01µm^2 particle size (n=3, *n.s.*). In addition, Early Endosome Antigen-1 (EEA1) was shown to be a marker of newly formed macropinosomes and mediated virus entry in cultured cells (Hamasaki, Araki, & Hatae, 2004; Sandgren et al., 2010). The protein sortin nexin-5 (SNX5) mediates macropinosome formation and is involved in its maturation (LIM, WANG, KERR, TEASDALE, & GLEESON, 2008). For this reason we analyzed co-localization of TBEV with endogenous EEA1 or SNX5 in Caco-2 cells. Figure 12D and 12E (Video S1 and S2) show a co-localization of TBEV E protein 24h p.i. with EEA1 or SNX5, respectively. Taken together, these findings indicate macropinocytosis as a mode of TBEV entry and internalization.

3.1.6 Translocation of TBEV via the paracellular pathway in the late phase of infection

During the transmission of TBEV by the oral route, virus may be released into the circulation after crossing the intestinal epithelium. To test this hypothesis, viruses were added to polarized Caco-2 cell monolayers that were grown on permeable filter supports for 3 weeks. Virus incubation was performed for 1h. Virus release into the basal medium was determined by measuring viral RNA copies over 5 days. As shown in Figure 13A, the amount of TBEV RNA copies in basal medium persistently increased in the course of infection, although TBEV was not detectable in the basal medium at 0h post infection. Simultaneously, TER was recorded, in order to determine, whether or not TBEV affects epithelial barrier function. Figure 13B shows that TER remained stable for 72h and decreased 4 days after infection.

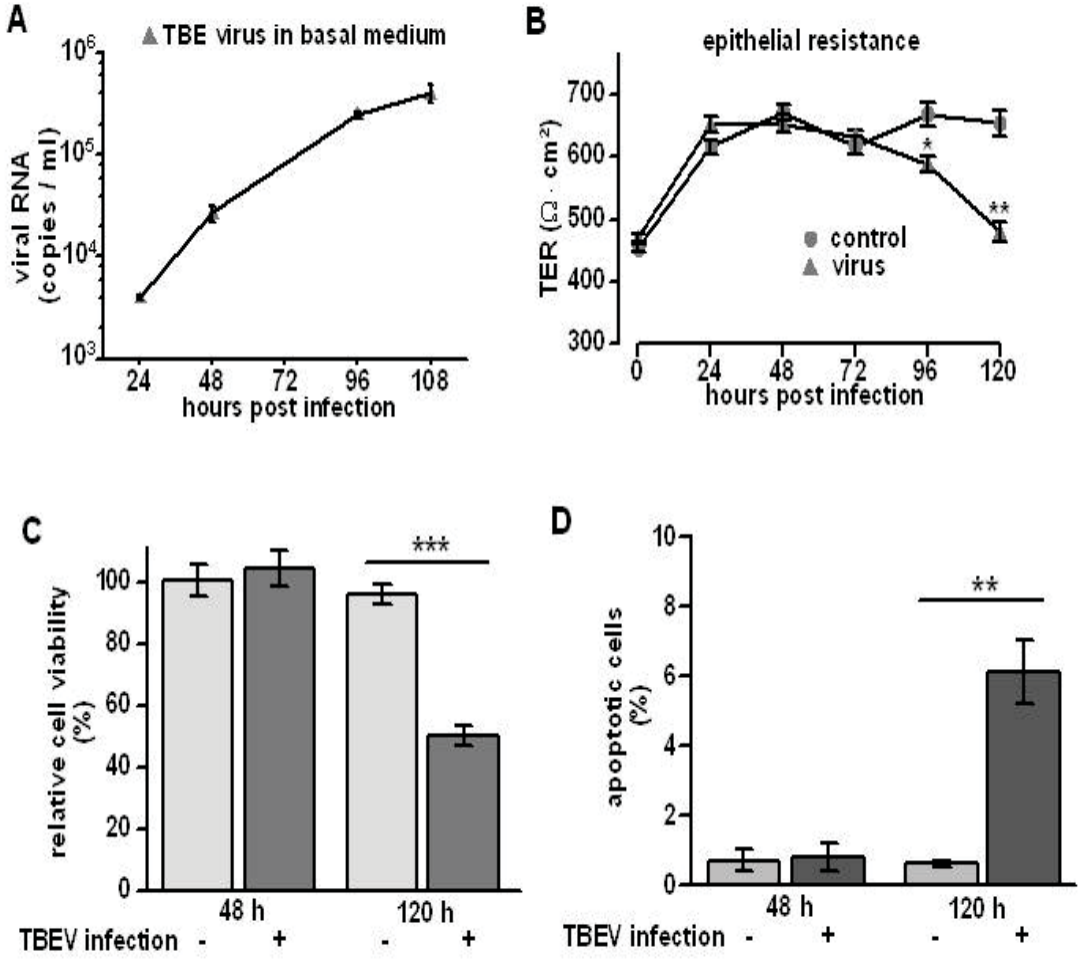

Figure 13. Translocation of TBEV through Caco-2 monolayers without affecting transepithelial electrical resistance (TER).
(A) Virus in basal medium. Polarized Caco-2 monolayers grown on permeable supports were infected with TBEV strain K23 from the apical surface. Viral RNA in each sample was detected by RT-qPCR. The data were displayed as mean with standard deviation. **(B)** Transepithelial electric resistance (TER) measurements during TBEV infection. Polarized Caco-2 monolayers grown on permeable supports were non-infected (triangles) or infected with TBEV K23 (circles) from the apical surface. TER values were measured from 0h to 120h post infection. n = 5, **P*<0.05, ***P*<0.01. **(C)** Cell viability during TBEV infection. Caco-2 cells were infected with TBEV strain K23 at a MOI of 1 and cell viability was analyzed by MTT assay. Cell viability was measured and calculated as a percentage of non-infected control cells. Data were expressed as mean ± standard error of the mean. **(D)** Analysis of TUNEL-positive cells. Confluent Caco-2 cells were infected with TBEV strain K23 and apoptosis was detected by a terminal deoxynucleotidyl transferase-mediated deoxyuridine triphosphate nick-end labeling (TUNEL) at 48h and 120h post infection. The ratios of TUNEL-postive cells to all cells were analyzed in 4 low-power fields from 3 independent samples of each group. ***P* < 0.01.

To exclude that lesions due to TBEV-induced cell death caused the translocation of the virus into the basal medium, cell viability was monitored by MTT assay. No change in cell viability was observed in the early phase of infection (until 2 days p.i.). However, 5 days p.i. cell viability decreased (Figure 13C). To corroborate these findings, TUNEL assays were performed to assess the apoptosis ratio in TBEV infected Caco-2 cells (Figure S1). 2 days p.i. the percentage of apoptotic cells was close to 0 and not different from untreated controls, but 5 days p.i. around 5% apoptotic cells were found (Figure 13D). These results suggest that TBEV significantly accelerated apoptosis in Caco-2 cells in the late phase of infection. Thus, in the early phase of infection (up to 2 days p.i.) no evidence for apoptosis induction was obtained and TER of the Caco-2 monolayers remained unaffected indicating an intact epithelial barrier. Therefore, virus translocation in the early phase of infection points to virus transcytosis. Whereas the decline in the integrity of the monolayer after 4 days p.i., as measured by a reduction in TER (Figure 13B) and an increase in apoptosis ratio (Figure 13D) as well as cytoskeletal (Figure 11A) and tight junction changes (Figure S2, Video S3), may be interpreted as hint for an additional route of virus translocation via the paracellular pathway.

3.2 Tick-borne encephalitis virus triggers inositol-requiring enzyme 1 (IRE1) and transcription factor 6 (ATF6) pathways of unfolded protein response

3.2.1 TBEV infection leads to induction of Hsp72 expression

Hsp72 protein is one of the newly identified components of UPRosome which interacts with IRE1α and regulates IRE1 signaling (Gupta et al., 2010). We first analyzed Hsp72 protein expression over the course of TBEV infection by immunofluorescence.

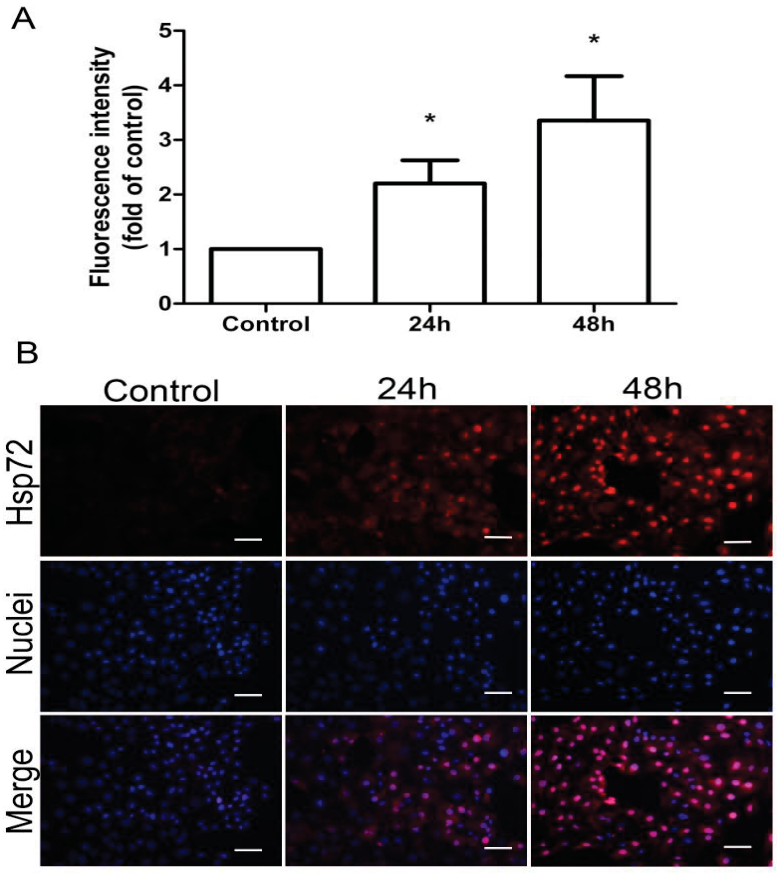

Figure 14. Increased Hsp72 expression in TBEV-infected cells.
(A) TBEV-infected Vero E6 cells were fixed and stained with anti-Hsp72 antibody and DAPI, respectively, at 24h and 48h post infection. Uninfected cells cultured for 48h were used as control. Images show intracellular Hsp72 (red) and cell nuclei (blue) by indirect immunofluorescence staining. Bar chart: 50μm. **(B)** The average Hsp72 fluorescence intensity calculated by the ImageJ software in each panel was compared with the control panel. The data were expressed as mean ± SD of three independent experiments. *: $P < 0.05$.

As shown in Figure 14A, Hsp72 protein expression was persistently increased during the course of infection compared to the control. It is also known that Hsp72 gains its chaperone capacity to deal with different stress situations by migrating to the nucleus (Knowlton, Grenier, Kirchhoff, & Salfity, 2000). Figure 14B shows that Hsp72 protein was mostly accumulated in the nucleus 48h post infection. These results suggest that Hsp72 might induce the IRE1 pathway during TBEV infection.

3.2.2 TBEV infection activates the IRE1 pathway

In the IRE1 pathway, active IRE1 truncates a 26-nucleotides intron from the unspliced XBP1 (uXBP1) mRNA and generates a cleaved form which encodes a highly active transcription factor, sXBP1 (Yoshida et al., 2001). To detect whether TBEV infection activates the IRE1 pathway, XBP1 mRNA was by RT-PCR using specific primer pairs. As expected, two forms of XBP1 mRNA were detected in the infected cells after virus infection, and a similar result was found in the TM-treated control cells (Figure 15A). In contrast, sXBP1 could not be detected in untreated and uninfected cells. The induction of sXBP1 apparently increased in TBEV-infected cells at 24h post infection (Figure 15B).

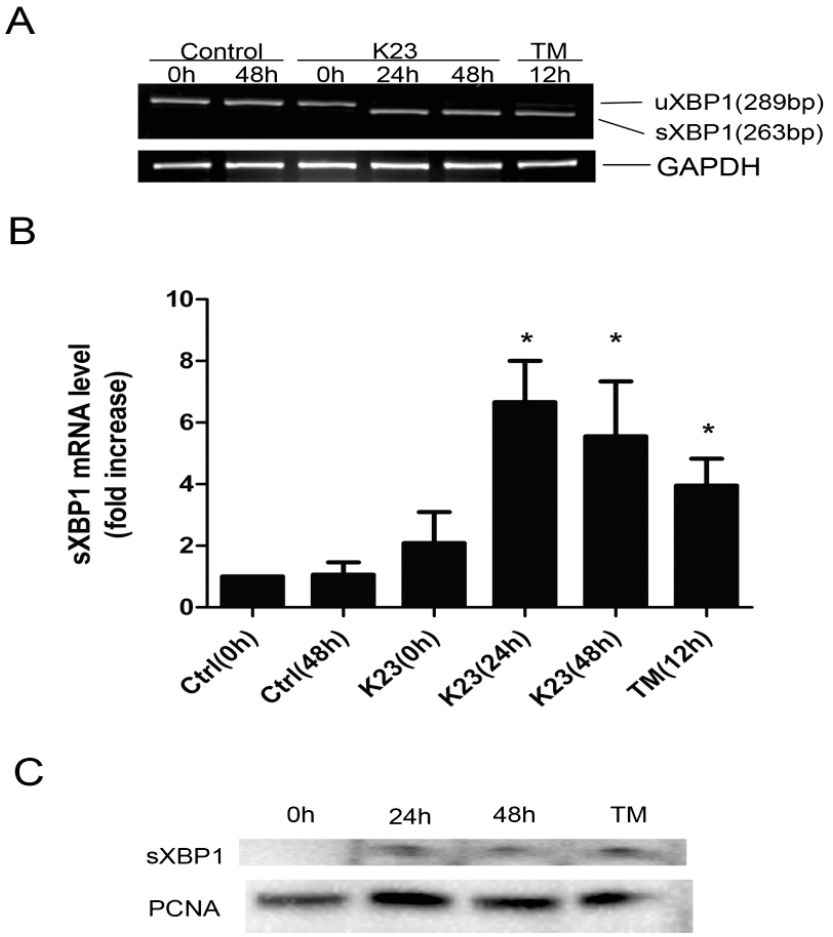

Figure 15. Induction of spliced XBP1 expression during TBEV infection.
(A) XBP1 mRNA was measured by RT-PCR. Vero E6 cells were either infected with TBEV strain K23 or treated with TM (1 µg/ml). XBP1 mRNA was amplified by RT-PCR using XBP1-specific primers. The products were separated by electrophoresis in 3% agarose gels and DNA was visualized by ethidium bromide. The unspliced XBP1 (uXBP1) mRNA was observed as a 289-bp band, and spliced XBP1 (sXBP1) mRNA was observed as a 263-bp band. TM was used as a positive control for the induction of sXBP1. GAPDH mRNA was used as loading control. The representative image was shown. **(B)** The band intensities of sXBP1 mRNA were measured by ImageJ software and expressed as fold increase compared to control (Ctrl 0h). *: $P < 0.05$. **(C)** Western blotting analysis of the spliced XBP1 expression. Nuclear extract were harvested at the indicated times post infection and analyzed by western blotting using an XBP1 antibody. TM treated cells were used as a positive control. The PCNA was used as a nuclear loading control. One of two representative results was shown.

Furthermore, the protein expression of sXBP1 in the nuclear fractions was at a high level detected by western blotting (Figure 15C). Moreover, activation of the IRE1 pathway could also be a mechanism to avoid cell death during virus

infection (Mishiba et al., 2013). We did not find apoptotic cells after TBEV infection at 24h post infection (Figure 16). All together, these results indicate that IRE1 pathway activated during TBEV infection.

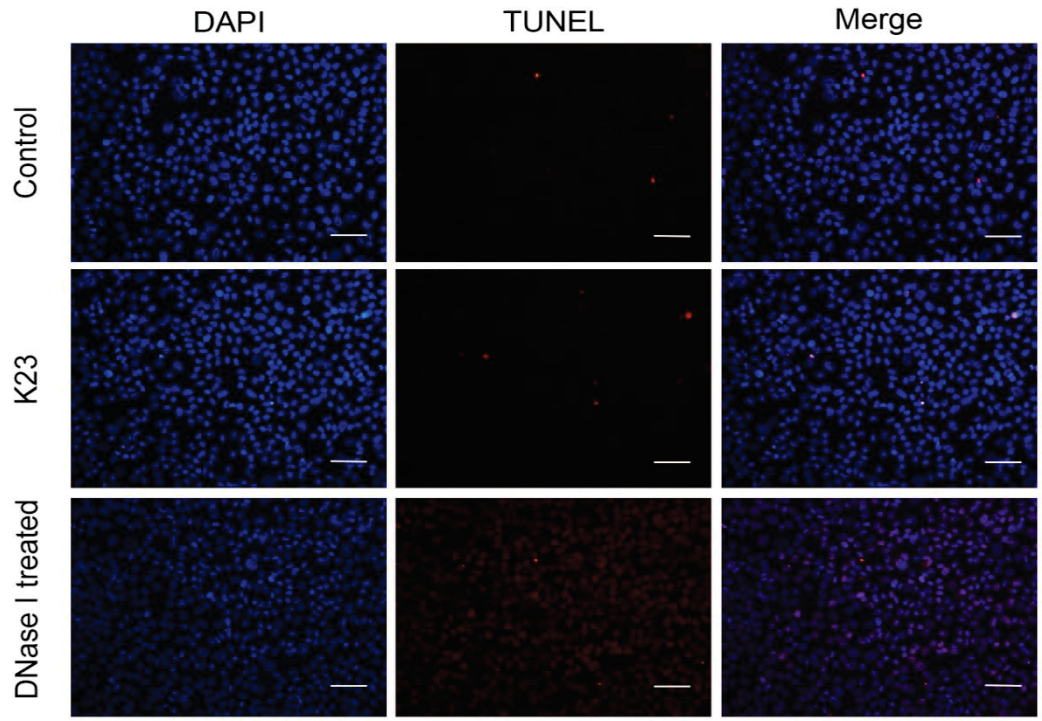

Figure 16. No signs of apoptosis in TBEV-infected Vero E6 cells.
Cells were infected with the TBEV and cultured for 48 h. Apoptosis was detected by a TUNEL assay. Nuclei stained with DAPI (blue). Samples incubated with DNase I (3000U/ml in 50 mM Tris-HCl, pH 7.5, 1mg/ml BSA) for 10min were used as positive control. Images were taken by a fluorescence microscope. Bar chart: 50μm.

3.2.3 TBEV infection activates the ATF6 pathway

As XBP1 is induced and regulated by ATF6 activation (K. Lee et al., 2002; Yoshida et al., 2001), we further investigated whether ATF6 was activated in TBEV-infected cells. During ATF6 activation, ATF6 translocates from the ER to the Golgi apparatus where it is processed by site-1 proteases (S1P) and site-2 proteases (S2P). The active fragment of ATF6 then translocates to the nucleus (Haze, Yoshida, Yanagi, Yura, & Mori, 1999). Cells transfected with a GFP-

ATF6 plasmid and infected with TBEV were used to test this hypothesis by immunofluorescence confocal microscopy.

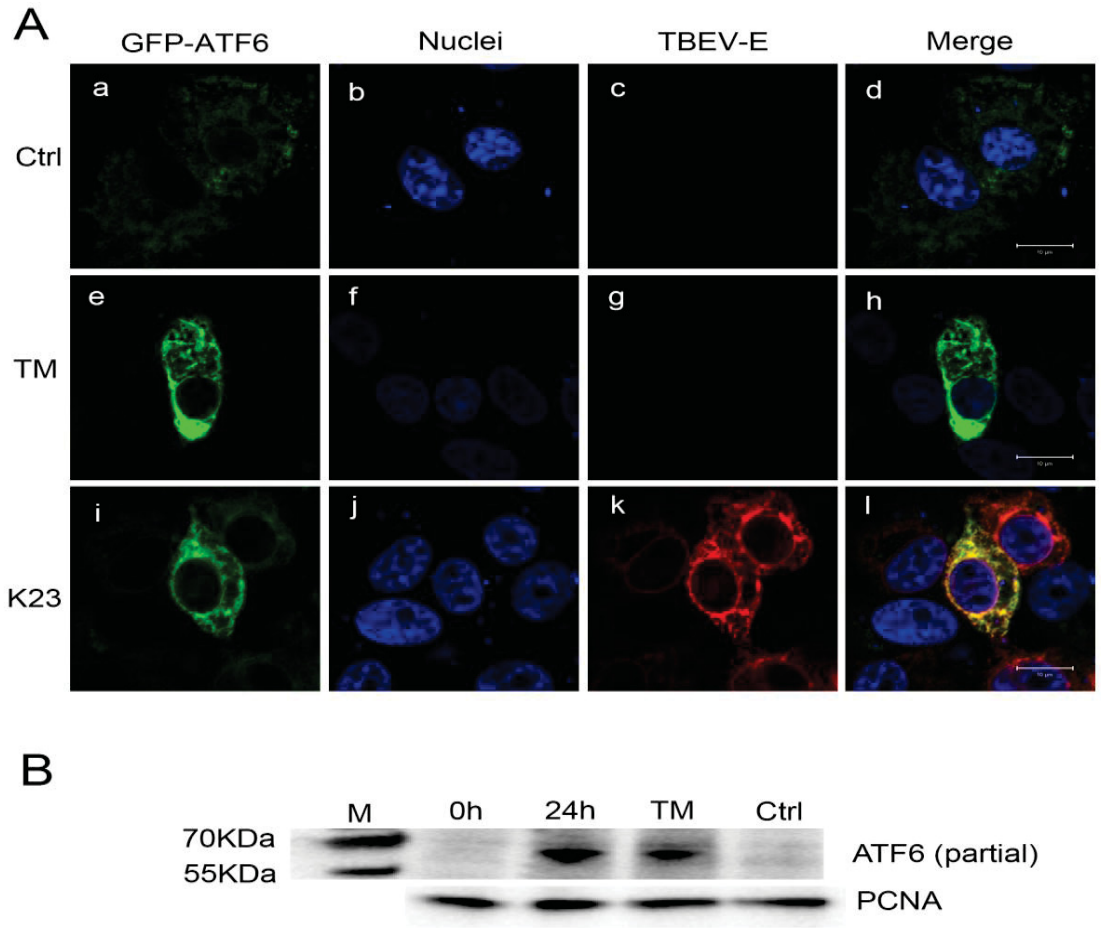

Figure 17. Analysis of ATF6 pathway during TBEV infection.
(A) Relocation of GFP-ATF6 during TBEV infection. GFP-ATF6 plasmids were transiently transfected into Vero E6 cells for 24h. Then the cells were infected with TBEV strain K23 and further cultured for 24h (panels i–l) or treated with TM (panels e–h) for 8h. Untreated and uninfected cells were used as controls (panels a–d). Confocal microscopy was used to detect GFP-ATF6 (green), TBEV E protein (red) and cell nuclei (blue). Bar chart: 10μm. **(B)** The expression of ATF6 cleavage from nucleus after TBEV infection was analyzed by western blotting. TM treated cells were used as a positive control for producing ATF6 cleavage. The PCNA was used as a nuclear loading control. One of two representative results was shown.

As shown in Figure 16A (panels a–d), GFP-ATF6 was evenly distributed in the cytoplasmatic ER-like structures and was not translocated to the nucleus in uninfected control cells. However, this characteristic distribution pattern

changed after TBEV infection. In Figure 16A (panels i–l) the TBEV-infected cells show an intense fluorescence near the nucleus, thus indicating that ATF6 is activated by TBEV infection. The same results were found in the TM-treated control cells in Figure 17A (panels e–h). We then confirmed these observations by monitoring the cleavage of ATF6 expression in the course of TBEV infection. Figure 17B demonstrated that an induction of ATF6 cleavage detected by western blotting. Taken together, these results show that TBEV infection induces the ATF6 pathway.

3.2.4 Inhibition of UPR pathway decreases TBEV replication

As the IRE1 pathway is activated by TBEV infection, we wanted to determine whether this pathway was a host antiviral response or facilitated virus replication. Therefore, we tested the effect of the IRE1 inhibitor, a newly identified inhibitor of the IRE1 pathway, on TBEV replication in TBEV-infected cells. In IRE1 inhibitor-pretreated cells the amount of infectious virus particles in the cell culture supernatant was significantly decreased compared to the untreated cells at 24h post infection. However, the amount of infectious virus particles in the cell culture supernatant was slightly increased at 48h post infection (Figure 18A). This phenomenon indicated that TBE virus may overcome or compensate the inhibition of IRE1 pathway by activation of ATF6 pathway and PERK pathway which need further confirmed. Also, western blot analysis revealed that the level of TBEV E-protein expression was reduced in the IRE1 inhibitor-treated cells (Figure 18C). Because of these results we wanted to know whether the inhibition of upstream signaling of all three UPR pathways might limit virus replication more efficiently. Therefore, we used the chemical chaperone and UPR inhibitor TUDCA. The inhibition assay was performed as described in the methods section. We observed a sharp decrease

of viral protein and infectious virus particles in TUDCA-pretreated cells (Figure 18B and 18D).

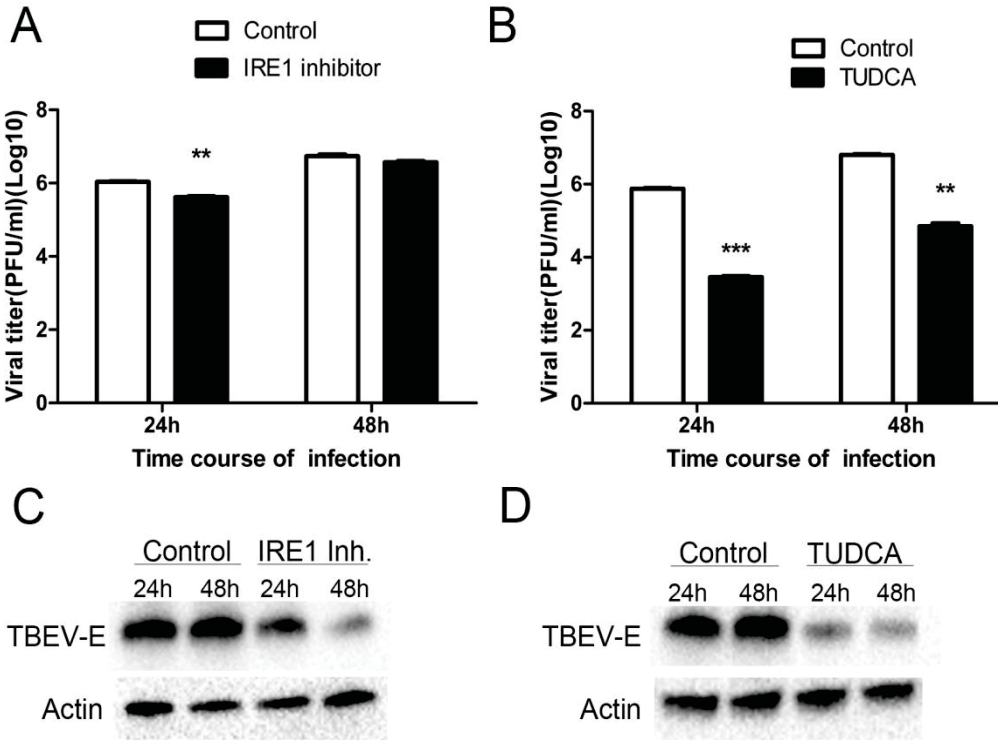

Figure 18. Effects of UPR inhibitors on the TBEV replication.
Vero E6 cells were treated with IRE1 inhibitor (60μM) or TUDCA (500μg/ml) for 1h and then infected with TBEV**. (A and B)** In the supernatant, virus titers were measured by plaque assay at 24h and 48h. The data represent the mean ± SD of three independent experiments. **(C and D)** Intracellular viral proteins were analyzed by western blot, and representative images were shown at 24h and 48h post infection. The virus titers with and without drug treatment at the indicated times were compared with Student's t test. **: $P < 0.01$; ***: $P < 0.001$.

In addition, MTT assay was used to rule out effects by pharmacological inhibition of ER stress on cell viability (Figure 18). Taken together, the results showed that inhibition of IRE1 pathway, especially inhibition of all three UPR pathways, decreased TBEV replication.

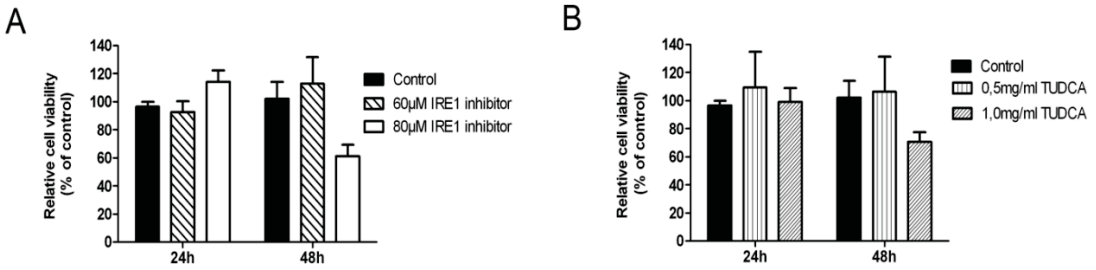

Figure 19. MTT assay with IRE1 inhibitor and TUDCA.
Caco-2 cells were treated with IRE1 inhibitor and TUDCA at different concentration separately (A and B). Cell viability was measured and calculated as a percentage to the control cells. Data were expressed with mean ± SD.

4. Discussion

4.1 Human intestinal Caco-2 cells are susceptible to TBEV infection

We found that human intestinal epithelial cells are susceptible to the TBEV infection and beneficial for its replication efficiently. The Caco-2 cell model, if grown for 3 weeks, is a suitable infection model for the small intestine, because it develops small intestine-like properties e.g. low transepithelial electrical resistances or expression of SGLT-1 sugar transporters. In our experiments TBEV replicates rapidly and after 2 days p.i. nearly all cells were infected although infectious dose was relatively low (MOI of 0.1). In the initial stage of infection up to 48h the Caco-2 cell monolayers' integrity remained stable as indicated by an unchanged TER, no induction of epithelial apoptosis and no obvious tight junction changes in IF stainings. This is in contrast to other viruses causing gastrointestinal (GI) symptoms e.g. experimental rotavirus infection in Caco-2 monolayers caused a rapid decrease of TER and a massive tight junction dysregulation within the first 24 h (Dickman et al., 2000).

4.2 TBEV is internalized into Caco-2 cells via macropinocytic pathway

The second important finding of this study was that macropinocytosis is an endocytic pathway in TBEV infection. Virus trafficking via macropinosomes was recently described for a growing number of viruses from other families such as echovirus (Krieger, Kim, Zhang, Marjomaki, & Bergelson, 2013), lentiviral HIV (Liu et al., 2002), or as reviewed for Vaccinia virus, Adenovirus 3, Coxsackievirus B, and Herpes simplex virus 1 etc. (Mercer & Helenius, 2009). Several lines of evidence indicate that the TBEV internalization by Caco-2 cells

is associated with macropinocytosis: (i) TBEV was detected in mid-sized vesicles of approximately 200 to 500 nm by EM in Caco-2 cells. These observations also revealed the virus particles probably assemble in the rER (Lorenz et al., 2003). (ii) Intracellular trafficking of TBEV containing vesicles was mediated by e.g. SNX5 signaling, which regulates the formation and maturation of macropinosomes [23]. Also EEA1 presented evidence for early endosomes in co-localization with TBEV. (iii) Inhibition of actin- or microtubule-dependent cytoskeleton polarization blocked virus particle trafficking and the inhibition of PI3K signaling also blocked virus uptake. (iv) Inhibition experiments with EIPA and fluid uptake assays of infected Caco-2 cells provide further evidence for a macropinocytosis mechanism. All these findings support the hypothesis that uptake of viral particles is mediated by the process of macropinocysis.

4.3 TBEV transmission to human by alimentary route

Since no experimental evidence showed how the flavivirus TBEV infect intestinal cells, we postulate that TBEV transmission and translocation into the organism takes place via the small intestine according to our experiment. In addition, oral experimental infection of animals resulted in a TBEV infection after an incubation time of several days (Pogodina, 1960; Van Tongeren, 1955). TBEV can resist to gastric juice [12]. It is reasonable that virus translocation via the small intestine is a possible route when humans consume unpasteurized milk products. Milk-borne infections and translocation across tight human epithelial barriers were also reported for other virus, such as Human T-cell leukemia virus (Martin-Latil et al., 2012). Furthermore, Human immunodeficiency virus transmission from maternal milk was shown (Read & American Academy of Pediatrics Committee on Pediatric, 2003). Milk as a

vehicle for pathogenic transmission is often observed and milk or its products protect pathogens to survive in the gastric acidic environment in order to get access to enterocytes. As the buffer capacity of milk and milk products is quite high, antibacterial or antiviral activity of the gastric juice is lowered when consuming milk, especially in young children or person with low gastric secretion (Bucker et al., 2012). Therefore, the gastric passage of pathogens (even in case of the gastric pathogen *Helicobacter pylori*) depends on the susceptibility of the hosts as well as on the type of the diet (Bucker et al., 2012).

4.4 Pathological changes in Caco-2 facilitate TBEV infection

In our experimental infection model, the beginning structural changes of the cytoskeleton and cytological changes in the early phase lead to further developed pathological changes in the late phase of infection. Although we cannot completely exclude virus translocation e.g. via apoptotic leaks, we found indications that the epithelium was (besides Cytological changes) not hampered in its integrity up to 48h p.i. Thus, we conclude that virus particles were released via exocytosis. However, after prolonged incubation time up to 5 days p.i. apoptosis ratio was massively increased in infected cell monolayers. Concomitantly, TER decreases after 4 days and was lowered to the half of the initial value at day 5. Therefore, paracellular virus translocation through the epithelial barrier may occur in the late phase of infection in the leaky epithelium. The induction of apoptosis by cytokine production, as shown for cytokine-containing supernatants of HIV-infected cells may also contribute to the barrier defect (Schmitz et al., 2002).

Moreover, we found additional pathological changes in late TBEV infection like the subcellular distribution of tight junction proteins in single areas of infected

Caco-2 monolayers that can promote virus translocation via the paracellular pathway (Figure S2). These kind of focal barrier defects were prominently observed in infection models of bacterial enteric pathogens e.g. *Yersinia enterocolitica* (Hering et al., 2011) or *Campylobacter concisus* (Nielsen et al., 2011). The drop in TER by TBEV can be assigned to the massive induction of apoptosis in the late phase of infection, but also re-distribution of barrier-forming tight junction proteins may contribute to the epithelial barrier defect. The lowered epithelial barrier function together with apoptosis induction gives rise to the view that GI symptoms as nausea, aches or vomiting were induced by the virus in the small intestine as shown for other viruses, e.g. astrovirus or HIV (Moser, Carter, & Schultz-Cherry, 2007; Schmitz et al., 2002). Pathological apoptosis induction can influence TER and increase permeability of the epithelium for macromolecules up to 4 kDa (Bojarski et al., 2001; Nielsen et al., 2011). Thus, a passive uptake mechanism into the organism for virus translocation and on the other hand the loss of solutes and water (diarrhea) is supposable a further pathogenic features of TBEV infection. Similarly, the pathogenic mechanisms in the human small intestine during norovirus infection could be described by epithelial apoptosis induction and tight junction dysregulation (Troeger et al., 2009). Moreover, the norovirus p20 protein showed interference with epithelial restitution mechanisms when stably transfected into HT-29/B6 colon cells (Hillenbrand et al., 2010). Likewise tight junction disruption caused by the capsid of the West Nile virus was found in Caco-2 monolayers (Medigeshi et al., 2009). From HIV infection it is known that the enteric immune cells were the site of virus progeny and that the HIV causes GI symptoms per se in the acute phase of infection (HIV enteropathy), thereby both apoptosis induction and tight junction changes contribute to the diarrhea

(Epple et al., 2010). Thus, it is supposable that the GI tract may also serve as the site for TBEV propagation and dissemination.

4.5 TBEV entering into host cells may depend on tight junction proteins

As TBEV can translocate via the transcellular as well as the paracellular pathway, the entry of the virus into the organism can lead to a systemic infection and subsequently infection of the nervous system. The mechanisms by which the viruses perturb the intestinal epithelial barrier by transcytosis and paracellular translocation (e.g. over apoptotic leaks) is also supposable for virus translocation through the endothelial blood-brain-barrier. The tight junction can be involved in virus endocytosis and replication. For example the Hepatitis C virus exploits the tight junction proteins occludin and claudin-1 as receptors for cell entry into liver cells (Ploss et al., 2009). In our cell model we did not find any co-localization of TBEV and tight junction or other apical membrane compartments such as lipid-rafts (data not shown), thus a cellular receptor for TBEV entry remains unknown. As Melik and co-workers reported that PDZ-domains may be important for TBEV replication and assembly (Melik et al., 2012), it is supposable that PDZ-motives of tight junction proteins (e.g. occludin) would be used by the virus and thereby tight junctional dysregulation may be induced. However, tight junction dysregulation by the virus has to be determined separately from apoptosis induction which can facilitate tight junction changes alone. For further research, the cellular defense mechanisms (clearance of virus particles) in low-dose TEBV-infected epithelial cells are worthwhile to proceed. In preliminary experiments low infectious doses did not affect epithelial integrity nor resulted in high replication rates as seen with MOI

above 0.1 (data not shown). Therefore, a possible transmission of TBEV between the cells via actin filament rearrangement should be considered for upcoming observations which seem to play an important role in TBEV infection (Burckhardt & Greber, 2009).

4.6 Activation of UPR by TBEV infection

Viruses have developed various strategies to exploit cellular host responses for their benefit and survival. In the whole cycle of virus replication, virus activates ER stress by producing viral double-stranded RNA intermediates and huge amounts of viral proteins (He, 2006). Due to their positive-sense genomic RNA, it is important for TBEV to use intracellular membranes to create a suitable microenvironment for replication. After viral particles bind to the cell surface, the viral RNA genomes are released into the cytoplasm and used for protein translation (Mandl, 2005). The process of TBEV assembly is detected by electron microscopy in the lumen of the ER and highly associated with cellular ER membrane rearrangements (Overby et al., 2010; Ruzek et al., 2009). Several flaviviruses including WNV, DENV and JEV can activate and regulate the UPR, a cellular stress response to alleviate ER stress caused by the accumulation of viral proteins; however, nothing is known about the regulation of the UPR in TBEV infection (Ambrose & Mackenzie, 2011; Klomporn, Panyasrivanit, Wikan, & Smith, 2011; Wu et al., 2011). In this study, we report for the first time that TBEV triggers the IRE1 pathway of the UPR, as the expression of spliced XBP1 mRNA and protein increased in TBEV-infected Vero E6 cells. Similar results were also observed in the course of JEV and DENV infections (Yu et al., 2006). In contrast, hepatitis C virus replicons inhibit the transactivation of XBP1, demonstrating the various pathogenic mechanisms

of different flaviviruses (Tardif, Mori, Kaufman, & Siddiqui, 2004). IRE1 pathway activation is downstream of ATF6 activation, and cleavage of ATF6 has been shown to up-regulate the level of XBP1 mRNA (K. Lee et al., 2002). The cleaved ATF6 moves from the ER to the Golgi complex and translocates to the nucleus. We demonstrated that activated ATF6 was accumulated near the nucleus of TBEV-infected cells. We then further confirmed the expression of cleaved ATF6 by western blotting which suggest that TBEV modulate the activation of the ATF6 pathway at the same time.

4.7 Inhibition of UPR decreases TBEV replication

The UPR is initiated to restore normal ER homeostasis during ER stress. Cell death occurs if the balance cannot be sustained (He, 2006). Activation of the IRE1 pathway may enhance the protein-folding ability which alleviates ER stress and reduces cytopathic effects during JEV and DV infection (Yu et al., 2006). In our experiments, we could not find apoptotic cells associated with TBEV infection. Thus, activation of the IRE1 pathway by TBEV could also be a mechanism to avoid cell death due to virus infection. Moreover, Hsp72, which is known to protect cells from ER stress (Gupta et al., 2010), is highly expressed in TBEV-infected cells. We also noticed nuclear accumulation of Hsp72 in TBEV-infected cells. This accumulation strengthens the resistance of cells to cellular death (Knowlton et al., 2000). Besides, it was shown for a close relative of TBEV, the hepatitis C virus, that overexpression of Hsp72 enhances viral RNA replication by increasing levels of the replicase complex (Chen et al., 2010). Taken together, we provide evidence that Hsp72 expression and XBP1 activation by TBEV may alleviate UPR which sustains the homeostasis against cell death and facilitates virus replication. Because spliced XBP1 is a

transcription factor regulating genes responsible for enhancing the protein-folding ability and facilitating the degradation of misfolded protein in the ER, the IRE1 pathway provides an adaptive capacity against ER stress (A. H. Lee, Iwakoshi, & Glimcher, 2003). We postulated that the IRE1 pathway induced by TBEV supports the cells in handling the ER stress and allows the virus to replicate more efficiently. This would mean inhibition of the UPR would decrease viral replication. Our results show that inhibition of the IRE1 pathway as well as inhibition of all three UPR pathways by IRE1 inhibitor or TUDCA, respectively, caused a reduction in viral titers. As the virus reduction in the TUDCA-treated cells was higher than that in the IRE1 inhibitor-treated cells, more than one UPR-signaling pathway might be involved in TBEV replication. Although the exact mechanisms of host and virus involved in XBP1 splicing and UPR activation have to be further investigated, we show here that TBEV initiated the IRE1 pathway and benefited from the cellular UPR. For this reason, inhibition of the UPR might be a novel option for a therapeutic treatment of TBE.

4.8 TBEV infection may involve in the UPR-mediated inflammation

Recent observations have shown that UPR initiates the inflammation response and regulates cytokine release (Zhang & Kaufman, 2008). TBEV invades the central nervous system by crossing the blood–brain barrier and then causes neural inflammation by its replication (Dumpis, Crook, & Oksi, 1999). However, TBEV rearranges intracellular membrane compartments and delays the release of inflammation cytokines which facilitate the virus entry into the central nervous system (Overby et al., 2010). UPR-induced inflammation-assisted or -restricted disease progression relies on many factors such as the cell type, disease stage

and type of ER sensors (Garg et al., 2012). Further studies in neural cells and mouse models with TBEV infection have to be performed to investigate the role of UPR-mediated inflammation in pathogenesis. Moreover, most TBE cases occur through a tick bite which delivers viruses into the host's circulation system. Dendritic cells are one of the most important cellular components which present antigen and initiate the adaptive immune response during virus invasion (Robertson, Mitzel, Taylor, Best, & Bloom, 2009). However, MHC class I molecules displayed on the cell surface of dendritic cells are impaired by the ER stress response (Granados et al., 2009; Ulianich et al., 2011). This phenomenon caused by ER stress response may be harmful for the dendritic cells presenting viral antigens and inhibit the host's antiviral response.

4.9 Conclusion

Taken together, TBEV is able to translocate through the intestinal epithelial barrier providing evidence that virus infection can occur via the alimentary route. In Caco-2 cell monolayers, TBEV entry into intestinal epithelial cells is mediated by macropinocytosis and replication of virus leads to high virus titers in apical and basal compartments. Future studies should confirm the findings on barrier breaking properties of TBEV infection on epithelial and endothelial borders in animal models and clinical observations.

In addition, my research showed that TBEV infection enhanced Hsp72 protein expression which regulates and enhances the IRE1 pathway. We then analyzed that TBEV infection induced the IRE1 pathway, which resulted in high expression of sXBP1. Moreover, we demonstrated that the translocation and expression of the cleaved ATF6, which indicated that ATF6 pathway activation during TBEV infection. Finally, we found that 3,5-Dibromosalicylaldehyde (IRE1

inhibitor) and tauroursodeoxycholic acid (TUDCA), two inhibitors of the UPR, impair TBEV replication. These findings provide new insights into the molecular mechanism of TBEV pathogenesis and may offer a new therapeutic approach to treat TBEV-induced diseases.

5. List of figures

6. List of Tables

7. Appendix

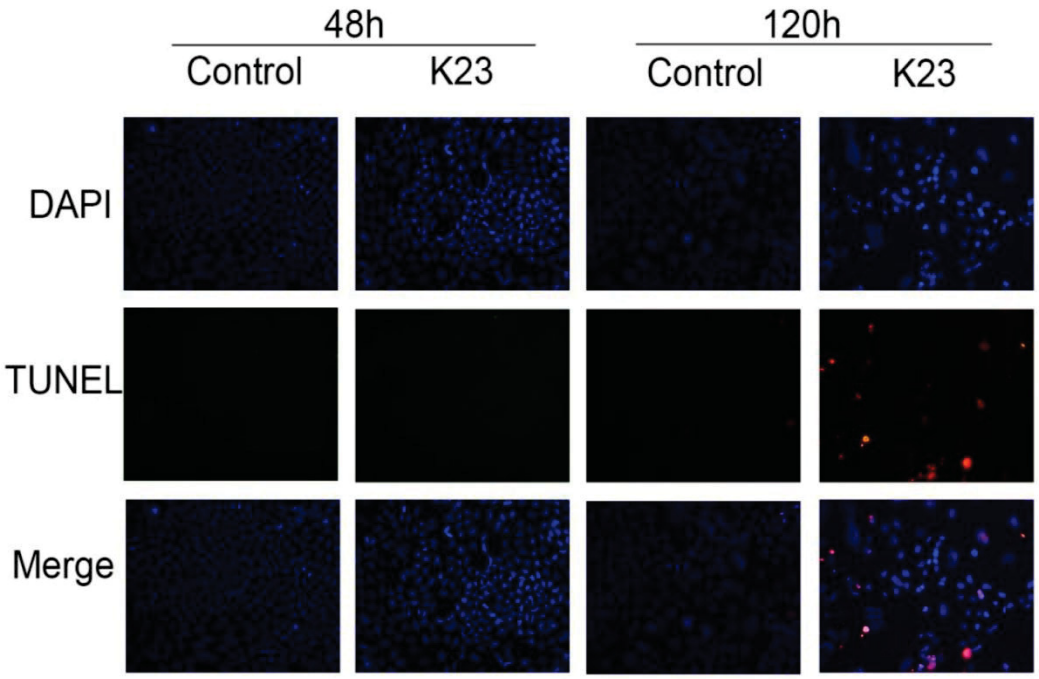

Figure S1. TUNEL assay in TBEV infected Caco-2 cells, supplementary to Figure 6D. Cellular apoptosis induced by TBEV infection. TUNEL assay in TBEV infected Caco-2 cells. Cells were infected with TBEV and apoptosis was detected by TUNEL (red) at 48 h and 120 h post infection. Cells were observed with the 20x objective (200x total magnification). Nuclei were stained with DAPI (blue). Micrographs were taken by fluorescence microscopy.

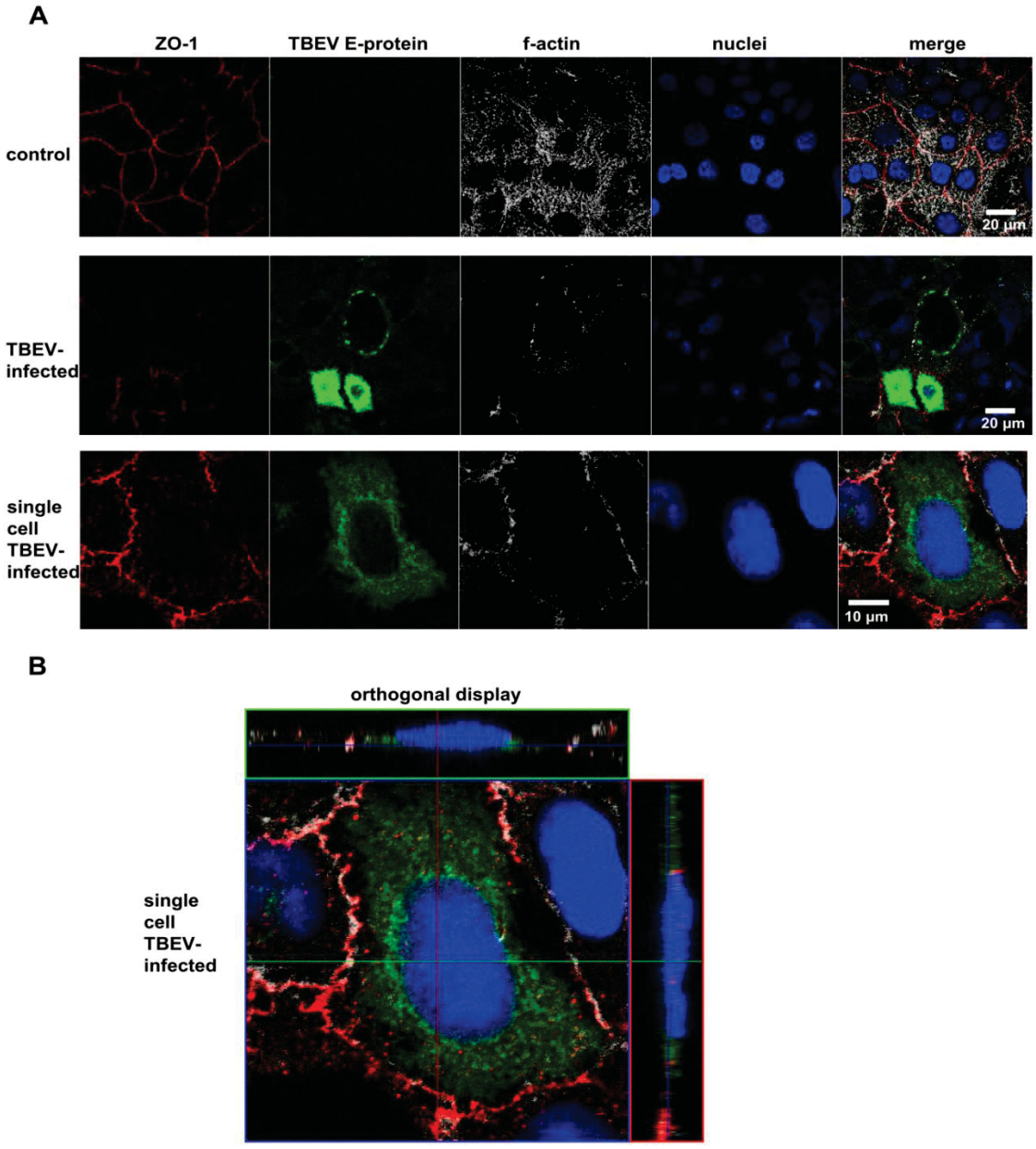

Figure S2. The effects of TBEV on tight junction changes may also contribute the drop in TER. Representative tight junction protein ZO-1 distribution and F-actin as cytoskeletal marker were stained in TBEV-infected and non-infected Caco-2 cells to display structural correlates to the electrophysiological findings. (A) ZO-1 and F-actin were disrupted by TBEV infection. Cells were fixed and stained for ZO-1 with primary antibodies and secondary anti-Rabbit Alexa Fluor 594 (red), TBEV E monoclonal antibody and anti- mouse conjugated with FITC (green). F-actin (white) stained with Atto-Phalloidin 647N (Sigma-Aldrich). Nuclei stained with DAPI (blue). Micrographs were taken by confocal microscopy. (B) Corresponding image of (A) as Z-stack in XY-plane.

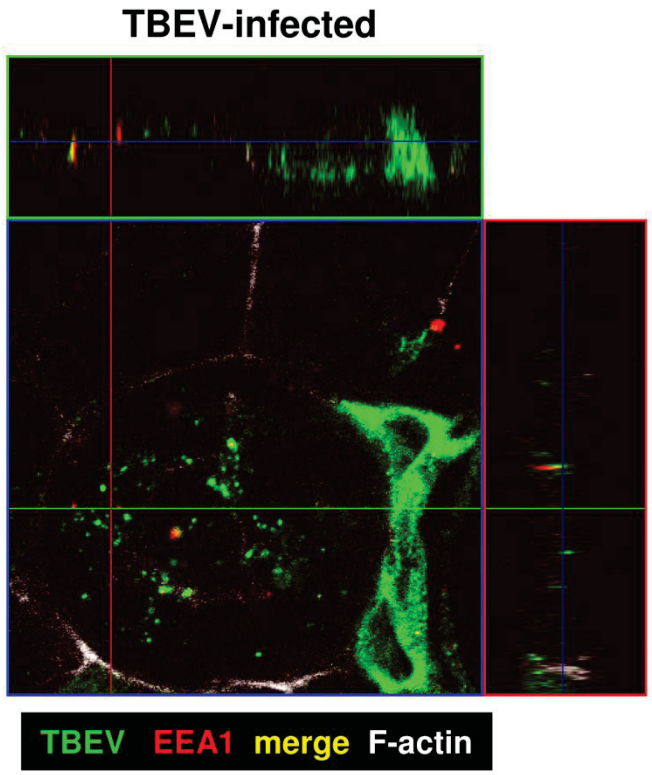

Figure S3 Co-localization of TBEV and EEA1. The infected cells were observed using confocal microscopy. The Z-stack image shows the virus co-localizes with EEA1 as yellow dots in XY-plane.

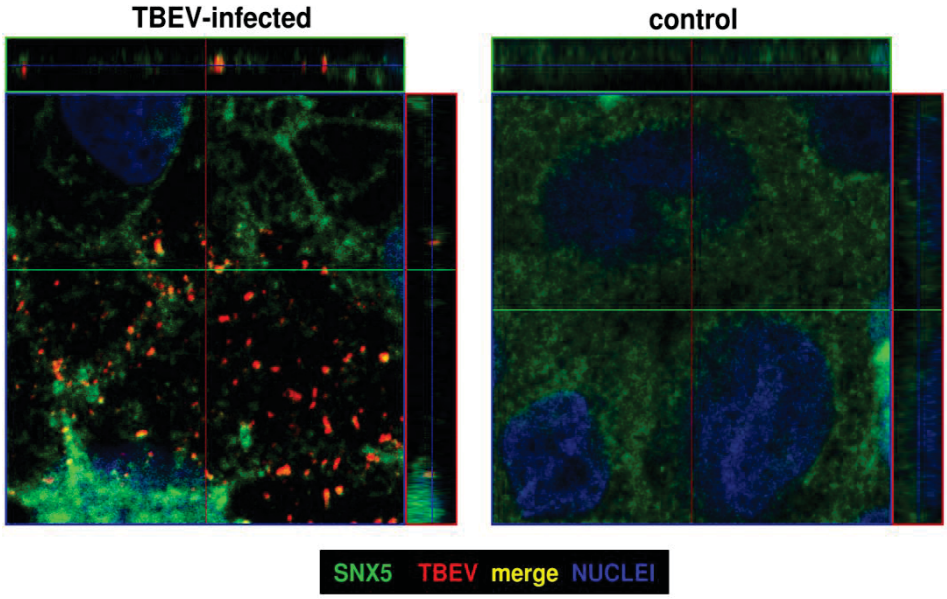

Figure S4. Co-localization of TBEV and SNX5. The Z-stack images in XY-plane were taken using confocal microscopy. The left image shows the virus co-localizes with SNX5 as yellow dots. In the right control image SNX5 is evenly distributed.

Video S1. Co-localization of TBEV and EEA1. Infected Caco-2 cells were observed using confocal microscopy and 3D video was created with Carl Zeiss LSM Image Examiner software. The moving 3D image shows the virus in co-localization with EEA1 as yellow dots.

Video S2. Co-localization of TBEV and SNX5. The moving 3D image shows the virus in co-localization with SNX5 as yellow dots.

Video S3. Tight junction changes induced by TBEV infection. The moving 3D image (from Supplemental Figure S2) shows that TBEV rearrange ZO1 distribution in affected regions of Caco-2 monolayers.

8. Reference

Achazi, K., Patel, P., Paliwal, R., Radonic, A., Niedrig, M., & Donoso-Mantke, O. (2012). RNA interference inhibits replication of tick-borne encephalitis virus in vitro. *Antiviral Res, 93*(1), 94-100. doi: 10.1016/j.antiviral.2011.10.023

Achazi, K., Ruzek, D., Donoso-Mantke, O., Schlegel, M., Ali, H. S., Wenk, M., . . . Niedrig, M. (2011). Rodents as sentinels for the prevalence of tick-borne encephalitis virus. *Vector Borne Zoonotic Dis, 11*(6), 641-647. doi: 10.1089/vbz.2010.0236

Allison, S. L., Schalich, J., Stiasny, K., Mandl, C. W., & Heinz, F. X. (2001). Mutational evidence for an internal fusion peptide in flavivirus envelope protein E. *J Virol, 75*(9), 4268-4275. doi: 10.1128/JVI.75.9.4268-4275.2001

Allison, S. L., Schalich, J., Stiasny, K., Mandl, C. W., Kunz, C., & Heinz, F. X. (1995). Oligomeric rearrangement of tick-borne encephalitis virus envelope proteins induced by an acidic pH. *J Virol, 69*(2), 695-700.

Ambrose, R. L., & Mackenzie, J. M. (2011). West Nile virus differentially modulates the unfolded protein response to facilitate replication and immune evasion. *J Virol, 85*(6), 2723-2732. doi: 10.1128/JVI.02050-10

Bakhvalova, V. N., Potapova, O. F., Panov, V. V., & Morozova, O. V. (2009). Vertical transmission of tick-borne encephalitis virus between generations of adapted reservoir small rodents. *Virus Res, 140*(1-2), 172-178. doi: 10.1016/j.virusres.2008.12.001

Balogh, Z., Egyed, L., Ferenczi, E., Ban, E., Szomor, K. N., Takacs, M., & Berencsi, G. (2012). Experimental infection of goats with tick-borne encephalitis virus and the possibilities to prevent virus transmission by raw goat milk. *Intervirology, 55*(3), 194-200. doi: 10.1159/000324023

Berger, E., & Haller, D. (2011). Structure-function analysis of the tertiary bile acid TUDCA for the resolution of endoplasmic reticulum stress in intestinal epithelial cells. *Biochem Biophys Res Commun, 409*(4), 610-615. doi: 10.1016/j.bbrc.2011.05.043

Best, S. M., Morris, K. L., Shannon, J. G., Robertson, S. J., Mitzel, D. N., Park, G. S., . . . Bloom, M. E. (2005). Inhibition of interferon-stimulated JAK-STAT signaling by a tick-borne flavivirus and identification of NS5 as an interferon antagonist. *J Virol, 79*(20), 12828-12839. doi: 10.1128/JVI.79.20.12828-12839.2005

Bojarski, C., Gitter, A. H., Bendfeldt, K., Mankertz, J., Schmitz, H., Wagner, S., . . . Schulzke, J. D. (2001). Permeability of human HT-29/B6 colonic epithelium as a function of apoptosis. *J Physiol, 535*(Pt 2), 541-552.

Bucker, R., Azevedo-Vethacke, M., Groll, C., Garten, D., Josenhans, C., Suerbaum, S., & Schreiber, S. (2012). Helicobacter pylori colonization critically depends on postprandial gastric conditions. *Sci Rep, 2*, 994. doi: 10.1038/srep00994

Burckhardt, C. J., & Greber, U. F. (2009). Virus movements on the plasma membrane support infection and transmission between cells. *PLoS Pathog, 5*(11), e1000621. doi: 10.1371/journal.ppat.1000621

Caini, S., Szomor, K., Ferenczi, E., Szekelyne Gaspar, A., Csohan, A., Krisztalovics, K., . . . Horvath, J. (2012). Tick-borne encephalitis transmitted by unpasteurised cow milk in western Hungary, September to October 2011. *Euro Surveill, 17*(12).

Charrel, R. N., Attoui, H., Butenko, A. M., Clegg, J. C., Deubel, V., Frolova, T. V., . . . de Lamballerie, X. (2004). Tick-borne virus diseases of human interest in Europe. *Clin Microbiol Infect, 10*(12), 1040-1055. doi: 10.1111/j.1469-0691.2004.01022.x

Chen, Y. J., Chen, Y. H., Chow, L. P., Tsai, Y. H., Chen, P. H., Huang, C. Y., . . . Hwang, L. H. (2010). Heat shock protein 72 is associated with the hepatitis C virus replicase complex and enhances viral RNA replication. *J Biol Chem, 285*(36), 28183-28190. doi: 10.1074/jbc.M110.118323

Cisak, E., Wojcik-Fatla, A., Zajac, V., Sroka, J., Buczek, A., & Dutkiewicz, J. (2010). Prevalence of tick-borne encephalitis virus (TBEV) in samples of raw milk taken randomly from cows, goats and sheep in eastern Poland. *Ann Agric Environ Med, 17*(2), 283-286.

Dickman, K. G., Hempson, S. J., Anderson, J., Lippe, S., Zhao, L., Burakoff, R., & Shaw, R. D. (2000). Rotavirus alters paracellular permeability and energy metabolism in Caco-2 cells. *Am J Physiol Gastrointest Liver Physiol, 279*(4), G757-766.

Dorrbecker, B., Dobler, G., Spiegel, M., & Hufert, F. T. (2010). Tick-borne encephalitis virus and the immune response of the mammalian host. *Travel Med Infect Dis, 8*(4), 213-222. doi: 10.1016/j.tmaid.2010.05.010

Dumpis, U., Crook, D., & Oksi, J. (1999). Tick-borne encephalitis. *Clin Infect Dis, 28*(4), 882-890. doi: 10.1086/515195

Ecker, M., Allison, S. L., Meixner, T., & Heinz, F. X. (1999). Sequence analysis and genetic classification of tick-borne encephalitis viruses from Europe and Asia. *J Gen Virol, 80 (Pt 1)*, 179-185.

Elshuber, S., Allison, S. L., Heinz, F. X., & Mandl, C. W. (2003). Cleavage of protein prM is necessary for infection of BHK-21 cells by tick-borne encephalitis virus. *J Gen Virol, 84*(Pt 1), 183-191.

Epple, H. J., Allers, K., Troger, H., Kuhl, A., Erben, U., Fromm, M., . . . Schneider, T. (2010). Acute HIV infection induces mucosal infiltration with CD4+ and CD8+ T cells, epithelial apoptosis, and a mucosal barrier defect. *Gastroenterology, 139*(4), 1289-1300. doi: 10.1053/j.gastro.2010.06.065

Garg, A. D., Kaczmarek, A., Krysko, O., Vandenabeele, P., Krysko, D. V., & Agostinis, P. (2012). ER stress-induced inflammation: does it aid or impede disease progression? *Trends Mol Med, 18*(10), 589-598. doi: 10.1016/j.molmed.2012.06.010

Gherman, C. M., Mihalca, A. D., Dumitrache, M. O., Gyorke, A., Oroian, I., Sandor, M., & Cozma, V. (2012). CO2 flagging - an improved method for the collection of questing ticks. *Parasit Vectors, 5*, 125. doi: 10.1186/1756-3305-5-125

Granados, D. P., Tanguay, P. L., Hardy, M. P., Caron, E., de Verteuil, D., Meloche, S., & Perreault, C. (2009). ER stress affects processing of MHC class I-associated peptides. *BMC Immunol, 10*, 10. doi: 10.1186/1471-2172-10-10

Gray, J. S., Dautel, H., Estrada-Pena, A., Kahl, O., & Lindgren, E. (2009). Effects of climate change on ticks and tick-borne diseases in europe. *Interdiscip Perspect Infect Dis, 2009*, 593232. doi: 10.1155/2009/593232

Gritsun, T. S., Lashkevich, V. A., & Gould, E. A. (2003). Tick-borne encephalitis. *Antiviral Res, 57*(1-2), 129-146.

Gupta, S., Deepti, A., Deegan, S., Lisbona, F., Hetz, C., & Samali, A. (2010). HSP72 protects cells from ER stress-induced apoptosis via enhancement of IRE1alpha-XBP1 signaling through a physical interaction. *PLoS Biol, 8*(7), e1000410. doi: 10.1371/journal.pbio.1000410

Haglund, M., & Gunther, G. (2003). Tick-borne encephalitis--pathogenesis, clinical course and long-term follow-up. *Vaccine, 21 Suppl 1*, S11-18.

Hamasaki, M., Araki, N., & Hatae, T. (2004). Association of early endosomal autoantigen 1 with macropinocytosis in EGF-stimulated A431 cells. *Anat Rec A Discov Mol Cell Evol Biol, 277*(2), 298-306. doi: 10.1002/ar.a.20027

Harding, H. P., Zhang, Y., & Ron, D. (1999). Protein translation and folding are coupled by an endoplasmic-reticulum-resident kinase. *Nature, 397*(6716), 271-274. doi: 10.1038/16729

Hayasaka, D., Ivanov, L., Leonova, G. N., Goto, A., Yoshii, K., Mizutani, T., . . . Takashima, I. (2001). Distribution and characterization of tick-borne encephalitis viruses from Siberia and far-eastern Asia. *J Gen Virol, 82*(Pt 6), 1319-1328.

Haze, K., Yoshida, H., Yanagi, H., Yura, T., & Mori, K. (1999). Mammalian transcription factor ATF6 is synthesized as a transmembrane protein and activated by

proteolysis in response to endoplasmic reticulum stress. *Mol Biol Cell, 10*(11), 3787-3799.
He, B. (2006). Viruses, endoplasmic reticulum stress, and interferon responses. *Cell Death Differ, 13*(3), 393-403. doi: 10.1038/sj.cdd.4401833
Heinz, F. X., Holzmann, H., Essl, A., & Kundi, M. (2007). Field effectiveness of vaccination against tick-borne encephalitis. *Vaccine, 25*(43), 7559-7567. doi: 10.1016/j.vaccine.2007.08.024
Heinz, F. X., Stiasny, K., Puschner-Auer, G., Holzmann, H., Allison, S. L., Mandl, C. W., & Kunz, C. (1994). Structural changes and functional control of the tick-borne encephalitis virus glycoprotein E by the heterodimeric association with protein prM. *Virology, 198*(1), 109-117. doi: 10.1006/viro.1994.1013
Hering, N. A., Richter, J. F., Krug, S. M., Gunzel, D., Fromm, A., Bohn, E., . . . Schulzke, J. D. (2011). Yersinia enterocolitica induces epithelial barrier dysfunction through regional tight junction changes in colonic HT-29/B6 cell monolayers. *Lab Invest, 91*(2), 310-324. doi: 10.1038/labinvest.2010.180
Hetz, C. (2012). The unfolded protein response: controlling cell fate decisions under ER stress and beyond. *Nat Rev Mol Cell Biol, 13*(2), 89-102. doi: 10.1038/nrm3270
Hillenbrand, B., Gunzel, D., Richter, J. F., Hohne, M., Schreier, E., Schulzke, J. D., & Mankertz, J. (2010). Norovirus non-structural protein p20 leads to impaired restitution of epithelial defects by inhibition of actin cytoskeleton remodelling. *Scand J Gastroenterol, 45*(11), 1307-1319. doi: 10.3109/00365521.2010.483013
Holzmann, H., Aberle, S. W., Stiasny, K., Werner, P., Mischak, A., Zainer, B., . . . Heinz, F. X. (2009). Tick-borne encephalitis from eating goat cheese in a mountain region of Austria. *Emerg Infect Dis, 15*(10), 1671-1673. doi: 10.3201/eid1510.090743
Hudopisk, N., Korva, M., Janet, E., Simetinger, M., Grgic-Vitek, M., Gubensek, J., . . . Avsic-Zupanc, T. (2013). Tick-borne encephalitis associated with consumption of raw goat milk, Slovenia, 2012. *Emerg Infect Dis, 19*(5), 806-808. doi: 10.3201/eid1905.121442
Janssens, S., & Beyaert, R. (2003). Role of Toll-like receptors in pathogen recognition. *Clin Microbiol Rev, 16*(4), 637-646.
Kaufmann, B., & Rossmann, M. G. (2011). Molecular mechanisms involved in the early steps of flavivirus cell entry. *Microbes Infect, 13*(1), 1-9. doi: 10.1016/j.micinf.2010.09.005
Kiffner, C., Vor, T., Hagedorn, P., Niedrig, M., & Ruhe, F. (2012). Determinants of tick-borne encephalitis virus antibody presence in roe deer (Capreolus capreolus) sera. *Med Vet Entomol, 26*(1), 18-25. doi: 10.1111/j.1365-2915.2011.00961.x
Kim, S. Y., Jeong, Y. E., Yun, S. M., Lee, I. Y., Han, M. G., & Ju, Y. R. (2009). Molecular evidence for tick-borne encephalitis virus in ticks in South Korea. *Med Vet Entomol, 23*(1), 15-20. doi: 10.1111/j.1365-2915.2008.00755.x
Kindberg, E., Vene, S., Mickiene, A., Lundkvist, A., Lindquist, L., & Svensson, L. (2011). A functional Toll-like receptor 3 gene (TLR3) may be a risk factor for tick-borne encephalitis virus (TBEV) infection. *J Infect Dis, 203*(4), 523-528. doi: 10.1093/infdis/jiq082
Klaus, C., Beer, M., Saier, R., Schau, U., Moog, U., Hoffmann, B., . . . Suss, J. (2012). Goats and sheep as sentinels for tick-borne encephalitis (TBE) virus--epidemiological studies in areas endemic and non-endemic for TBE virus in Germany. *Ticks Tick Borne Dis, 3*(1), 27-37. doi: 10.1016/j.ttbdis.2011.09.011
Klaus, C., Horugel, U., Hoffmann, B., & Beer, M. (2013). Tick-borne encephalitis virus (TBEV) infection in horses: clinical and laboratory findings and epidemiological investigations. *Vet Microbiol, 163*(3-4), 368-372. doi: 10.1016/j.vetmic.2012.12.041

Klomporn, P., Panyasrivanit, M., Wikan, N., & Smith, D. R. (2011). Dengue infection of monocytic cells activates ER stress pathways, but apoptosis is induced through both extrinsic and intrinsic pathways. *Virology, 409*(2), 189-197. doi: 10.1016/j.virol.2010.10.010

Knowlton, A. A., Grenier, M., Kirchhoff, S. R., & Salfity, M. (2000). Phosphorylation at tyrosine-524 influences nuclear accumulation of HSP72 with heat stress. *Am J Physiol Heart Circ Physiol, 278*(6), H2143-2149.

Koivusalo, M., Welch, C., Hayashi, H., Scott, C. C., Kim, M., Alexander, T., . . . Grinstein, S. (2010). Amiloride inhibits macropinocytosis by lowering submembranous pH and preventing Rac1 and Cdc42 signaling. *J Cell Biol, 188*(4), 547-563. doi: 10.1083/jcb.200908086

Kozlovskaya, L. I., Osolodkin, D. I., Shevtsova, A. S., Romanova, L., Rogova, Y. V., Dzhivanian, T. I., . . . Karganova, G. G. (2010). GAG-binding variants of tick-borne encephalitis virus. *Virology, 398*(2), 262-272. doi: 10.1016/j.virol.2009.12.012

Krieger, S. E., Kim, C., Zhang, L., Marjomaki, V., & Bergelson, J. M. (2013). Echovirus 1 entry into polarized Caco-2 cells depends on dynamin, cholesterol, and cellular factors associated with macropinocytosis. *J Virol*. doi: 10.1128/JVI.03415-12

Kurisaki, K., Kurisaki, A., Valcourt, U., Terentiev, A. A., Pardali, K., Ten Dijke, P., . . . Moustakas, A. (2003). Nuclear factor YY1 inhibits transforming growth factor beta- and bone morphogenetic protein-induced cell differentiation. *Mol Cell Biol, 23*(13), 4494-4510.

Labuda, M., Austyn, J. M., Zuffova, E., Kozuch, O., Fuchsberger, N., Lysy, J., & Nuttall, P. A. (1996). Importance of localized skin infection in tick-borne encephalitis virus transmission. *Virology, 219*(2), 357-366. doi: 10.1006/viro.1996.0261

Laue, M. (2010). Electron microscopy of viruses. *Methods Cell Biol, 96*, 1-20. doi: 10.1016/S0091-679X(10)96001-9

Lee, A. H., Iwakoshi, N. N., & Glimcher, L. H. (2003). XBP-1 regulates a subset of endoplasmic reticulum resident chaperone genes in the unfolded protein response. *Mol Cell Biol, 23*(21), 7448-7459.

Lee, K., Tirasophon, W., Shen, X., Michalak, M., Prywes, R., Okada, T., . . . Kaufman, R. J. (2002). IRE1-mediated unconventional mRNA splicing and S2P-mediated ATF6 cleavage merge to regulate XBP1 in signaling the unfolded protein response. *Genes Dev, 16*(4), 452-466. doi: 10.1101/gad.964702

Leonova, G. N., & Pavlenko, E. V. (2009). Characterization of neutralizing antibodies to Far Eastern of tick-borne encephalitis virus subtype and the antibody avidity for four tick-borne encephalitis vaccines in human. *Vaccine, 27*(21), 2899-2904. doi: 10.1016/j.vaccine.2009.02.069

Lim, J. P., Wang, J. T., Kerr, M. C., Teasdale, R. D., & Gleeson, P. A. (2008). A role for SNX5 in the regulation of macropinocytosis. *BMC Cell Biol, 9*, 58. doi: 10.1186/1471-2121-9-58

Lin, J. H., Walter, P., & Yen, T. S. (2008). Endoplasmic reticulum stress in disease pathogenesis. *Annu Rev Pathol, 3*, 399-425. doi: 10.1146/annurev.pathmechdis.3.121806.151434

Lindquist, L., & Vapalahti, O. (2008). Tick-borne encephalitis. *Lancet, 371*(9627), 1861-1871. doi: 10.1016/S0140-6736(08)60800-4

Liu, N. Q., Lossinsky, A. S., Popik, W., Li, X., Gujuluva, C., Kriederman, B., . . . Fiala, M. (2002). Human immunodeficiency virus type 1 enters brain microvascular endothelia by macropinocytosis dependent on lipid rafts and the mitogen-activated protein kinase signaling pathway. *J Virol, 76*(13), 6689-6700.

Lorenz, I. C., Kartenbeck, J., Mezzacasa, A., Allison, S. L., Heinz, F. X., & Helenius, A. (2003). Intracellular assembly and secretion of recombinant subviral particles from tick-borne encephalitis virus. *J Virol, 77*(7), 4370-4382.

Lu, Z., Broker, M., & Liang, G. (2008). Tick-borne encephalitis in mainland China. *Vector Borne Zoonotic Dis, 8*(5), 713-720. doi: 10.1089/vbz.2008.0028
Mandl, C. W. (2005). Steps of the tick-borne encephalitis virus replication cycle that affect neuropathogenesis. *Virus Res, 111*(2), 161-174. doi: 10.1016/j.virusres.2005.04.007
Mandl, C. W., Kroschewski, H., Allison, S. L., Kofler, R., Holzmann, H., Meixner, T., & Heinz, F. X. (2001). Adaptation of tick-borne encephalitis virus to BHK-21 cells results in the formation of multiple heparan sulfate binding sites in the envelope protein and attenuation in vivo. *J Virol, 75*(12), 5627-5637. doi: 10.1128/JVI.75.12.5627-5637.2001
Marciniak, S. J., Yun, C. Y., Oyadomari, S., Novoa, I., Zhang, Y., Jungreis, R., . . . Ron, D. (2004). CHOP induces death by promoting protein synthesis and oxidation in the stressed endoplasmic reticulum. *Genes Dev, 18*(24), 3066-3077. doi: 10.1101/gad.1250704
Martin-Latil, S., Gnadig, N. F., Mallet, A., Desdouits, M., Guivel-Benhassine, F., Jeannin, P., . . . Ceccaldi, P. E. (2012). Transcytosis of HTLV-1 across a tight human epithelial barrier and infection of subepithelial dendritic cells. *Blood, 120*(3), 572-580. doi: 10.1182/blood-2011-08-374637
Medigeshi, G. R., Hirsch, A. J., Brien, J. D., Uhrlaub, J. L., Mason, P. W., Wiley, C., . . . Nelson, J. A. (2009). West nile virus capsid degradation of claudin proteins disrupts epithelial barrier function. *J Virol, 83*(12), 6125-6134. doi: 10.1128/JVI.02617-08
Medigeshi, G. R., Lancaster, A. M., Hirsch, A. J., Briese, T., Lipkin, W. I., Defilippis, V., . . . Nelson, J. A. (2007). West Nile virus infection activates the unfolded protein response, leading to CHOP induction and apoptosis. *J Virol, 81*(20), 10849-10860. doi: 10.1128/JVI.01151-07
Medlock, J. M., Hansford, K. M., Bormane, A., Derdakova, M., Estrada-Pena, A., George, J. C., . . . Van Bortel, W. (2013). Driving forces for changes in geographical distribution of Ixodes ricinus ticks in Europe. *Parasit Vectors, 6*, 1. doi: 10.1186/1756-3305-6-1
Melik, W., Ellencrona, K., Wigerius, M., Hedstrom, C., Elvang, A., & Johansson, M. (2012). Two PDZ binding motifs within NS5 have roles in Tick-borne encephalitis virus replication. *Virus Res, 169*(1), 54-62. doi: 10.1016/j.virusres.2012.07.001
Mercer, J., & Helenius, A. (2009). Virus entry by macropinocytosis. *Nat Cell Biol, 11*(5), 510-520. doi: 10.1038/ncb0509-510
Miorin, L., Romero-Brey, I., Maiuri, P., Hoppe, S., Krijnse-Locker, J., Bartenschlager, R., & Marcello, A. (2013). Three-dimensional architecture of tick-borne encephalitis virus replication sites and trafficking of the replicated RNA. *J Virol, 87*(11), 6469-6481. doi: 10.1128/JVI.03456-12
Mishiba, K., Nagashima, Y., Suzuki, E., Hayashi, N., Ogata, Y., Shimada, Y., & Koizumi, N. (2013). Defects in IRE1 enhance cell death and fail to degrade mRNAs encoding secretory pathway proteins in the Arabidopsis unfolded protein response. *Proc Natl Acad Sci U S A, 110*(14), 5713-5718. doi: 10.1073/pnas.1219047110
Moser, L. A., Carter, M., & Schultz-Cherry, S. (2007). Astrovirus increases epithelial barrier permeability independently of viral replication. *J Virol, 81*(21), 11937-11945. doi: 10.1128/JVI.00942-07
Mukhopadhyay, S., Kuhn, R. J., & Rossmann, M. G. (2005). A structural perspective of the flavivirus life cycle. *Nat Rev Microbiol, 3*(1), 13-22. doi: 10.1038/nrmicro1067
Niedrig, M., Klockmann, U., Lang, W., Roeder, J., Burk, S., Modrow, S., & Pauli, G. (1994). Monoclonal antibodies directed against tick-borne encephalitis virus with neutralizing activity in vivo. *Acta Virol, 38*(3), 141-149.

Nielsen, H. L., Nielsen, H., Ejlertsen, T., Engberg, J., Gunzel, D., Zeitz, M., . . . Bucker, R. (2011). Oral and fecal Campylobacter concisus strains perturb barrier function by apoptosis induction in HT-29/B6 intestinal epithelial cells. *PLoS One, 6*(8), e23858. doi: 10.1371/journal.pone.0023858

Orlinger, K. K., Hofmeister, Y., Fritz, R., Holzer, G. W., Falkner, F. G., Unger, B., . . . Kreil, T. R. (2011). A tick-borne encephalitis virus vaccine based on the European prototype strain induces broadly reactive cross-neutralizing antibodies in humans. *J Infect Dis, 203*(11), 1556-1564. doi: 10.1093/infdis/jir122

Overby, A. K., Popov, V. L., Niedrig, M., & Weber, F. (2010). Tick-borne encephalitis virus delays interferon induction and hides its double-stranded RNA in intracellular membrane vesicles. *J Virol, 84*(17), 8470-8483. doi: 10.1128/JVI.00176-10

Palus, M., Vojtiskova, J., Salat, J., Kopecky, J., Grubhoffer, L., Lipoldova, M., . . . Ruzek, D. (2013). Mice with different susceptibility to tick-borne encephalitis virus infection show selective neutralizing antibody response and inflammatory reaction in the central nervous system. *J Neuroinflammation, 10*, 77. doi: 10.1186/1742-2094-10-77

Pfaffle, M., Littwin, N., Muders, S. V., & Petney, T. N. (2013). The ecology of tick-borne diseases. *Int J Parasitol, 43*(12-13), 1059-1077. doi: 10.1016/j.ijpara.2013.06.009

Pfeffer, M., & Dobler, G. (2011). Tick-borne encephalitis virus in dogs--is this an issue? *Parasit Vectors, 4*, 59. doi: 10.1186/1756-3305-4-59

Ploss, A., Evans, M. J., Gaysinskaya, V. A., Panis, M., You, H., de Jong, Y. P., & Rice, C. M. (2009). Human occludin is a hepatitis C virus entry factor required for infection of mouse cells. *Nature, 457*(7231), 882-886. doi: 10.1038/nature07684

Pogodina, V. V. (1958). [Resistance of tick-borne encephalitis virus to gastric juice]. *Vopr Virusol, 3*(5), 271-275.

Pogodina, V. V. (1960). [An experimental study on the pathogenesis of tick-borne encephalitis following alimentary infection. Part 2. A study of the methods of excretion of viruses from the body of the white mouse]. *Vopr Virusol, 5*, 279-285.

Read, J. S., & American Academy of Pediatrics Committee on Pediatric, A. (2003). Human milk, breastfeeding, and transmission of human immunodeficiency virus type 1 in the United States. American Academy of Pediatrics Committee on Pediatric AIDS. *Pediatrics, 112*(5), 1196-1205.

Rey, F. A., Heinz, F. X., Mandl, C., Kunz, C., & Harrison, S. C. (1995). The envelope glycoprotein from tick-borne encephalitis virus at 2 A resolution. *Nature, 375*(6529), 291-298. doi: 10.1038/375291a0

Robertson, S. J., Mitzel, D. N., Taylor, R. T., Best, S. M., & Bloom, M. E. (2009). Tick-borne flaviviruses: dissecting host immune responses and virus countermeasures. *Immunol Res, 43*(1-3), 172-186. doi: 10.1007/s12026-008-8065-6

Roelandt, S., Heyman, P., De Filette, M., Vene, S., Van der Stede, Y., Caij, A. B., . . . Roels, S. (2011). Tick-borne encephalitis virus seropositive dog detected in Belgium: screening of the canine population as sentinels for public health. *Vector Borne Zoonotic Dis, 11*(10), 1371-1376. doi: 10.1089/vbz.2011.0647

Ron, D., & Walter, P. (2007). Signal integration in the endoplasmic reticulum unfolded protein response. *Nat Rev Mol Cell Biol, 8*(7), 519-529. doi: 10.1038/nrm2199

Rushton, J. O., Lecollinet, S., Hubalek, Z., Svobodova, P., Lussy, H., & Nowotny, N. (2013). Tick-borne encephalitis virus in horses, Austria, 2011. *Emerg Infect Dis, 19*(4), 635-637. doi: 10.3201/eid1904.121450

Ruzek, D., Salat, J., Singh, S. K., & Kopecky, J. (2011). Breakdown of the blood-brain barrier during tick-borne encephalitis in mice is not dependent on CD8+ T-cells. *PLoS One, 6*(5), e20472. doi: 10.1371/journal.pone.0020472

Ruzek, D., Vancova, M., Tesarova, M., Ahantarig, A., Kopecky, J., & Grubhoffer, L. (2009). Morphological changes in human neural cells following tick-borne encephalitis virus infection. *J Gen Virol, 90*(Pt 7), 1649-1658. doi: 10.1099/vir.0.010058-0

Samali, A., Fitzgerald, U., Deegan, S., & Gupta, S. (2010). Methods for monitoring endoplasmic reticulum stress and the unfolded protein response. *Int J Cell Biol, 2010*, 830307. doi: 10.1155/2010/830307

Sandgren, K. J., Wilkinson, J., Miranda-Saksena, M., McInerney, G. M., Byth-Wilson, K., Robinson, P. J., & Cunningham, A. L. (2010). A differential role for macropinocytosis in mediating entry of the two forms of vaccinia virus into dendritic cells. *PLoS Pathog, 6*(4), e1000866. doi: 10.1371/journal.ppat.1000866

Schmitz, H., Rokos, K., Florian, P., Gitter, A. H., Fromm, M., Scholz, P., . . . Schulzke, J. D. (2002). Supernatants of HIV-infected immune cells affect the barrier function of human HT-29/B6 intestinal epithelial cells. *AIDS, 16*(7), 983-991.

Si, B. Y., Jiang, T., Zhang, Y., Deng, Y. Q., Huo, Q. B., Zheng, Y. C., . . . Zhu, Q. Y. (2011). Complete genome sequence analysis of tick-borne encephalitis viruses isolated in northeastern China. *Arch Virol, 156*(8), 1485-1488. doi: 10.1007/s00705-011-1031-y

Stetson, D. B., & Medzhitov, R. (2006). Type I interferons in host defense. *Immunity, 25*(3), 373-381. doi: 10.1016/j.immuni.2006.08.007

Su, H. L., Liao, C. L., & Lin, Y. L. (2002). Japanese encephalitis virus infection initiates endoplasmic reticulum stress and an unfolded protein response. *J Virol, 76*(9), 4162-4171.

Tardif, K. D., Mori, K., Kaufman, R. J., & Siddiqui, A. (2004). Hepatitis C virus suppresses the IRE1-XBP1 pathway of the unfolded protein response. *J Biol Chem, 279*(17), 17158-17164. doi: 10.1074/jbc.M312144200

Troeger, H., Loddenkemper, C., Schneider, T., Schreier, E., Epple, H. J., Zeitz, M., . . . Schulzke, J. D. (2009). Structural and functional changes of the duodenum in human norovirus infection. *Gut, 58*(8), 1070-1077. doi: 10.1136/gut.2008.160150

Ulianich, L., Terrazzano, G., Annunziatella, M., Ruggiero, G., Beguinot, F., & Di Jeso, B. (2011). ER stress impairs MHC Class I surface expression and increases susceptibility of thyroid cells to NK-mediated cytotoxicity. *Biochim Biophys Acta, 1812*(4), 431-438. doi: 10.1016/j.bbadis.2010.12.013

Umareddy, I., Pluquet, O., Wang, Q. Y., Vasudevan, S. G., Chevet, E., & Gu, F. (2007). Dengue virus serotype infection specifies the activation of the unfolded protein response. *Virol J, 4*, 91. doi: 10.1186/1743-422X-4-91

Van Tongeren, H. A. (1955). Encephalitis in Austria. IV. Excretion of virus by milk of the experimentally infected goat. *Arch Gesamte Virusforsch, 6*(2-3), 158-162.

Vazquez, M., Muehlenbein, C., Cartter, M., Hayes, E. B., Ertel, S., & Shapiro, E. D. (2008). Effectiveness of personal protective measures to prevent Lyme disease. *Emerg Infect Dis, 14*(2), 210-216. doi: 10.3201/eid1402.070725

Volkmann, K., Lucas, J. L., Vuga, D., Wang, X., Brumm, D., Stiles, C., . . . Patterson, J. B. (2011). Potent and selective inhibitors of the inositol-requiring enzyme 1 endoribonuclease. *J Biol Chem, 286*(14), 12743-12755. doi: 10.1074/jbc.M110.199737

Werme, K., Wigerius, M., & Johansson, M. (2008). Tick-borne encephalitis virus NS5 associates with membrane protein scribble and impairs interferon-stimulated JAK-STAT signalling. *Cell Microbiol, 10*(3), 696-712. doi: 10.1111/j.1462-5822.2007.01076.x

Wu, Y. P., Chang, C. M., Hung, C. Y., Tsai, M. C., Schuyler, S. C., & Wang, R. Y. (2011). Japanese encephalitis virus co-opts the ER-stress response protein GRP78 for viral infectivity. *Virol J, 8*, 128. doi: 10.1186/1743-422X-8-128

Ye, J., Rawson, R. B., Komuro, R., Chen, X., Dave, U. P., Prywes, R., . . . Goldstein, J. L. (2000). ER stress induces cleavage of membrane-bound ATF6 by the same proteases that process SREBPs. *Mol Cell, 6*(6), 1355-1364.

Yoshida, H., Matsui, T., Yamamoto, A., Okada, T., & Mori, K. (2001). XBP1 mRNA is induced by ATF6 and spliced by IRE1 in response to ER stress to produce a highly active transcription factor. *Cell, 107*(7), 881-891.

Yoshii, K., Mottate, K., Omori-Urabe, Y., Chiba, Y., Seto, T., Sanada, T., . . . Takashima, I. (2011). Epizootiological study of tick-borne encephalitis virus infection in Japan. *J Vet Med Sci, 73*(3), 409-412.

Yu, C. Y., Hsu, Y. W., Liao, C. L., & Lin, Y. L. (2006). Flavivirus infection activates the XBP1 pathway of the unfolded protein response to cope with endoplasmic reticulum stress. *J Virol, 80*(23), 11868-11880. doi: 10.1128/JVI.00879-06

Yun, S. M., Kim, S. Y., Ju, Y. R., Han, M. G., Jeong, Y. E., & Ryou, J. (2011). First complete genomic characterization of two tick-borne encephalitis virus isolates obtained from wild rodents in South Korea. *Virus Genes, 42*(3), 307-316. doi: 10.1007/s11262-011-0575-y

Zhang, K., & Kaufman, R. J. (2008). From endoplasmic-reticulum stress to the inflammatory response. *Nature, 454*(7203), 455-462. doi: 10.1038/nature07203

Acknowledgments

This work would have not been able to accomplish without the help of colleagues, friends, and family. Although there are many of them I cannot acknowledge each contribution by name, I would like to thank everyone who support me through this challenging as well as interesting time.

First, I appreciate my supervisor Prof. Matthias Niedrig deeply, who not only provided me an opportunity to do my PhD study in his group but also offered a very good research platform and freedom environment. I would also like to thank him for his constructive comments on my PhD work and thesis.

I would also like to thank Dr. Christoph Curth to introduce me the laser scanning microscopy and Dr. Kazimierz Madela for his perfect technical support. Many thanks to Lars Möller for his support in EM and provided me with many meaningful EM images.

Thanks to Dr. Roland Bücker for his scientific ideas and persistent support in performing the experiments. Special thanks to Prof. Jörg-Dieter Schulzke for his critical comments in writing publication. Special thanks to Prof. Detlev H. Krüger for his useful comments and support. Thanks to Dr. Regina Schaedler for helping me with the German abstract of this thesis.

In addition, I also want to thank the present and past memebers of Prof. Matthais Niedrig's group (Dr. Nadine Litzba, Nina Stock, Dr. Peter Hagedorn, Ravish Paliwal, Dr. Pranav Patel, Dia Roy, Dr. Cristina Domingo Carrasco, Escadafal, Camille, Anette Teichmann, Patricia Bußmann, Petra Kreher, Marion Mielke, Dr. Oliver Donoso Mantke, Dr. Katharina Achazi, Yessica Schulze and Dr. Sonja Linke), that give me the scientific ideas, technique assistances, as well as warm friendship in the laboratory and daily life.

Finally, I want to express my deep appreciation to my families: my mother has been encouraging me with her support which let me to pursue my dream; my wife, Xin Chen, with her love, care and understanding, has been giving me an important power to conquer any obstacles that I met although she lives in China lonely for these years; my brother and my sister always kindly picked me up and gave me a warm welcome when I had holidays in China.

List of Publications

1. **Yu, C.**, K. Achazi, and M. Niedrig, *Tick-borne encephalitis virus triggers inositol-requiring enzyme 1 (IRE1) and transcription factor 6 (ATF6) pathways of unfolded protein response.* Virus Res, 2013. 178(2): p. 471-7.
2. **Yu, C.**, **K. Achazi**, M. Lars, JD. Schulzke, M. Niedrig, R. Bücker, *Tick-borne encephalitis virus replication, intracellular trafficking, and pathogenicity in human intestinal Caco-2 cell monolayers.* Plos ONE, accepted.

Conference and workshop participation

1. Yu, C., R. Bücker, K. Achazi, M. Niedrig, *Human Intestinal Caco-2 cells are Susceptible to Tick-borne Encephalitis Virus Infection.* National Symposium on Zoonoses Research, 11-12 October 2012 in Berlin, Germany; poster presentation**.**

2. Yu, C., K. Achazi, and M. Niedrig, *Blockage of inositol-requiring enzyme 1 (IRE1) pathway prevents tick-borne encephalitis virus replication.* National Symposium on Zoonoses Research, 19-20 September 2013 in Berlin, Germany; poster presentation.